

University of South Bohemia, České Budějovice  
Faculty of Sciences

**Establishment of novel test systems for standardized  
screening of bioactive Substances**

Ph.D. Thesis

**Dipl.Biol. Maren Pflüger**

Supervisor: Prof. RNDr. Rüdiger Etrich PhD  
University of South Bohemia, České Budějovice  
and  
Institute of Nanobiology and Structural Biology, Global Change Research Center,  
Academy of Sciences of the Czech Republic

Co-Supervisor: Prof. Harald Hundsberger  
University of Applied Science Krems, Krems an der Donau

Krems an der Donau 2013



This thesis should be cited as:

**Pflüger M.**, 2013: Establishment of novel test systems for standardized screening of bioactive Substances. Ph.D. thesis, University of South Bohemia, Faculty of Science, České Budějovice, Czech Republic, 48 pp.

## **Annotation**

Bioactive substances, isolated from nature are a promising source of compounds for the pharmaceutical industry. The pre-selection of bioactivity is already done by environmental evolution which is an advantage compared to the time consuming random screening of synthetic drugs. For the identification and characterization of bioactive substances cell based *in vitro* test systems are important for the routine-based search. Therefore it is necessary to compare and characterize commercial assays for their ability to test substances for cytotoxicity, anti-inflammatory or wound healing effects in high-throughput assays.

## **Declaration [in Czech]**

Prohlašuji, že svoji disertační práci jsem vypracoval samostatně pouze s použitím pramenů a literatury uvedených v seznamu citované literatury.

Prohlašuji, že v souladu s § 47b zákona č. 111/1998 Sb. v platném znění souhlasím se zveřejněním své disertační práce, a to v úpravě vzniklé vypuštěním vyznačených částí archivovaných Přírodovědeckou fakultou elektronickou cestou ve veřejně přístupné části databáze STAG provozované Jihočeskou univerzitou v Českých Budějovicích na jejích internetových stránkách, a to se zachováním mého autorského práva k odevzdanému textu této kvalifikační práce. Souhlasím dále s tím, aby toutéž elektronickou cestou byly v souladu s uvedeným ustanovením zákona č. 111/1998 Sb. zveřejněny posudky školitele a oponentů práce i záznam o průběhu a výsledku obhajoby kvalifikační práce. Rovněž souhlasím s porovnáním textu mé kvalifikační práce s databází kvalifikačních prací Theses.cz provozovanou Národním registrem vysokoškolských kvalifikačních prací a systémem na odhalování plagiátů.

*V Kreamsu dne 10.9. 2013*

.....

Maren Pflüger

This thesis originated from a partnership of the University of South Bohemia in České Budějovice, and the University of Applied Science KREMS, supporting doctoral studies in the biophysics study programme. All experimental work was undertaken at the Department of Biotechnology, University of Applied Science KREMS.



Přírodovědecká  
fakulta  
Faculty  
of Science



FH KREMS  
UNIVERSITY OF APPLIED  
SCIENCES / AUSTRIA

### **Financial support**

This work was funded by the European Territorial Co-operation grant (M00140) and the Österreichische Forschungsförderungsgesellschaft (FFG, 821021, 822710).

## **Acknowledgement**

Foremost I want to thank my supervisor Prof. RNDr. Rüdiger Ettrich PhD for providing me with the opportunity to complete my PhD thesis at the University of South Bohemia and the Academy of Sciences of the Czech Republic in Nové Hradý as an external student at the University of Applied Science in Krems. Further I want to thank my internal supervisor Prof.(FH) Mag. Dr. Harald Hundberger and the whole team of the University of Applied Science in Krems for their support to made my thesis work possible.

I would like to show my gratitude to my former colleague and supervisor Prof.(FH) Dr.Christoph Wiesner for his enthusiasm, encouragement and support of my research work.

Especially I want to thank my former supervisor Rudolph Lucas Ph.D. who helped me to start my doctoral research at the University of Applied Science Krems for his contribution in time, ideas and suggestions for my work.

I want to thank our co-operation partner, particularly Ing. Jiří Kopecký, CSc. and Aleksandra Kapuscik in Czech Republic from the Institute of Microbiology, Department of Phototrophic microorganisms, Academy of Sciences in Třeboň for their work in culturing, extraction and purification of the cyanobacterial compounds.

And finally, but not least, thanks goes to my whole family, who have been an important and indispensable source of spiritual support.

## List of relevant publications and author's contribution

**Maren Pflüger**, Aleksandra Kapuscik, Rudolf Lucas, Anita Koppensteiner, Michael Katzlinger, Jouni Jokela, Andreas Eger, Nico Jacobi, Christoph Wiesner, Elisabeth Hofmann, Kamil Önder, Jiri Kopecky, Wolfgang Schütt, and Harald Hundsberger, A (2013) Combined Impedance and AlphaLISABased Approach to Identify Antiinflammatory and Barrier-Protective Compounds in Human Endothelium, *Journal of Biomolecular Screening*, 18, 66-73, DOI: 10.1177/1087057112458316 (IF = 2.089)

*MP conducted the AlphaLisa measurements and analyzed the cyanobacterial compounds for anti-inflammatory capabilities. MP processed the data and wrote the manuscript.*

Vineeta Khare, Alex Lyakhovich, Kyle Dammanna, Michaela Lang, Melanie Borgmann, Boris Tichy, Sarka Pospisilova, Gloria Luciani, Christoph Campregher, Rayko Evstatiev, **Maren Pflueger**, Harald Hundsberger, Christoph Gasche (2013) Mesalamine modulates intercellular adhesion through inhibition of p-21 activated kinase-1; *Biochemical Pharmacology*, 85 234–244 (IF = 4.529)

*MP performed Electrical cell-substrate impedance sensing measurements for the analysing of the cell adhesion capabilities of Mesalamine and revised the manuscript.*

Machicao F, Muresanu DF, Hundsberger H, **Pflüger M**, Guekht A, (2012) Pleiotropic neuroprotective and metabolic effects of Actovegin's mode of action, *Journal of the Neurological Sciences*, 322(1-2):222-7, DOI: 10.1016/j.jns.2012.07.069 (IF = 2.413)

*MP conducted the potential of Actovegin to modulate the NF- $\kappa$ B pathway on the CellSensor® human embryonic kidney cell line, NF- $\kappa$ B-bla HEK 293T and analyzed the recorded data.*

Kreiseder B, Orel L, Bujnow C, Buschek S, **Pflueger M**, Schuett W, Hundsberger H, de Martin R, Wiesner C, (2013)  $\alpha$ -Catulin downregulates E-cadherin and

promotes melanoma progression and invasion, *International Journal of Cancer*, 132(3):521-30, DOI: 10.1002/ijc.27698 (IF = 6.198)

*MP conducted the Luciferase measurements, performed migration assays and analyzed the reported data.*

S Amatschek, R Lucas, A Eger, **M Pflueger**, H Hundsberger, C Knoll, S Grosse-Kracht, W Schuett, F Koszik, D Maurer and C Wiesner (2010) CXCL9 induces chemotaxis, chemorepulsion and endothelial barrier disruption through CXCR3-mediated activation of melanoma cells, *British Journal of Cancer*, 104, 469 – 479 (IF = 5.082)

*MP performed Transwell/transendothelial migration assays and the Electrical cell-substrate impedance sensing measurements, processed the data and revised the manuscript.*

Christoph Wiesner, **Maren Pflüger**, Jiri Kopecky, Dalibor Stys, Barbara Entler, Rudolf Lucas, Harald Hundsberger, Wolfgang Schütt (2008) Implementation of ECIS technology for the characterization of potential therapeutic drugs that promote wound-healing, *GMS Krankenhaushygiene Interdisziplinär*, Vol. 3(1), ISSN 1863-5245 (Not in WOS)

*MP conducted the Electrical cell-substrate impedance sensing measurements for the screening for wound healing activities of cyanobacterial compounds, analyzed the data and revised the manuscript.*

Harald Hundsberger, Alexander Verin, Christoph Wiesner, **Maren Pflüger**, Alexander Dulebo, Wolfgang Schütt, Ignace Lasters, Daniela N. Männel, Albrecht Wendel and Rudolf Lucas (2008) TNF: a Moonlighting Protein at the Interface between Cancer and Infection, *Frontiers in Bioscience*, 13:5374-86, DOI: 10.2741/3087 (IF = 3.52)

*MP conducted the measurements for analyzing the lectin-like domain of TNF and processed the data.*

Christoph Wiesner, Jiri Kopecky, **Maren Pflueger**, Harald Hundsberger, Barbara Entler, Christoph Kleber, Josef Atzler, Pavel Hrouzek, Dalibor Stys, Alena Lukesova, Wolfgang Schuett and Rudolf Lucas (2007) Endothelial Cell-Based Methods for the Detection of Cyanobacterial Anti- Inflammatory and Wound-Healing Promoting Metabolites, *Drug Metabolism Letters*, 1, 254-260 (IF = 1.315)

*MP performed the Cell-based Elisas for ICAM-1 expression, analyzed the data and revised the manuscript.*

Rudolf Lucas, Harald Hundsberger, **Maren Pflüger**, Bernhard Fischer, Denis Morel, Clemens Braun, Albrecht Wendel, Trinad Chakraborty, Wolfgang Schütt, Christoph Wiesner and Jürg Hamacher (2007) The Tumor Necrosis Factor-derived TIP peptide: a potential anti-edema drug, *Letters in Drug Design & Discovery*, Vol. 4, 336- 340 (IF = 0.87)

*MP conducted the sodium uptake in Ussing chamber measurements and analyzed the data.*



## Abbreviations

AlphaScreen: Amplified Luminescent Proximity Homogeneous Assay

AP1: activator protein-1

ASK1: apoptosis signal-regulating kinase 1

BAFF: B-cell activating factor (BAFF)

CCF4-AM: chloro-hydroxycoumarin fluorescein - acetoxymethyl

CMV: cytomegalovirus

DMEM: Dulbecco's Modified Eagle's Medium

DNA: Deoxyribonucleic acid

ECIS: Electrical Cell substrate Impedances Sensing

EMT: epithelial-mesenchymal transition

FADD: Fas-associated protein with death domain

FBS: Fetal Bovine Serum

GFP: green fluorescence protein

HaCaT: Human adult low Calcium high Temperature Keratinocytes

HEPES: 4-(2-Hydroxyethyl) piperazine-1-ethanesulfonic acid

HLMVEC: Human lung microvascular endothelial cell

hTNF: human Tumor necrosis factor

Huvec: Human umbilical vein endothelial cells

IKK: I $\kappa$ B kinase

IL-8: Interleukin 8

Jnk pathway: c-Jun N-terminal kinase pathway

LOCI: Luminescent Oxygen Channeling Immunoassay

MAPK: the map kinase

MEKK: Map/Erk kinase kinase

NEAA: Nonessential Amino Acid

NF- $\kappa$ B: Nuclear Factor kappa B

NIH-3T3: National Institutes of Health- "3 day transfer, inoculum  $3 \times 10^5$  cells"

PBS: Phosphate buffered saline

RIP: receptor interacting protein

ROS: Reactive Oxygen Species

RPMI: Roswell Park Memorial Institute

Stat3: signal transducer activator of transcription-3

TRADD: TNF receptor-associated protein with death domain

TRAF: TNFR associated factor

TR-FRET: Time-Resolved Fluorescence Resonance Energy Transfer

VEGF: Vascular endothelial growth factor

---

Wehi: Walter and Eliza Hall Institute

## List of Figures

|   |    |
|---|----|
| FIGURE 1 HALLMARKS OF CANCER WITH THERAPEUTIC TARGETS (11)  | 4  |
| FIGURE 2 TUMOR NECROSIS FACTOR ALPHA PATHWAY AND THE ALTERNATIVE NF-KB PATHWAY  | 5  |
| FIGURE 3 ALPHALISA TECHNOLOGY   | 8  |
| FIGURE 4 GENEBLAZER® PRINCIPLE (28) LANTHASCREEEN® TECHNOLOGY   | 9  |
| FIGURE 5 LANTHASCREEEN® PRINCIPLE (28)  | 10 |
| FIGURE 6 EVALUATION OF THE CYTOTOXICITY OF SEVERAL CYANOBACTERIAL COMPOUNDS   | 21 |
| FIGURE 7 CYTOTOXICITY MEASUREMENT OF NOSTOC SP. DE NO.114   | 22 |
| FIGURE 8 CYTOTOXICITY MEASUREMENT OF NOSTOC SP. NO.17 AND NO.8, CALU1533 NO.183 AND NOSTOC MUSCORUM NO.30               | 23 |
| FIGURE 9 CYTOTOXICITY MEASUREMENT OF NOSTOC STRAIN NO.8   | 24 |
| FIGURE 10 CYANOBACTERIAL COMPOUNDS (NOSTOC) WERE TESTED FOR CYTOTOXICITY AND MULTIPLEXED TO DETECT APOPTOSIS INDUCTION. | 25 |
| FIGURE 11 MEASUREMENT OF CYTOTOXICITY OF CYANOBACTERIAL COMPOUND N122 M/Z 872.5 WITH MULTITOX-FLUOR™.                   | 26 |
| FIGURE 12 CYTOTOXICITY MEASUREMENT OF SEVERAL CRUDE EXTRACTS ISOLATED FROM CYANOBACTERIA                                | 27 |
| FIGURE 13 MEASUREMENT OF THE IMPEDANCE AFTER TRITONX-100 TREATMENT.   | 28 |
| FIGURE 14 MEASUREMENT OF THE IMPEDANCE AFTER STIMULATION OF HLMVECS WITH NOSTOC SP. NO.17                               | 28 |
| FIGURE 15 RESPONSE RATIO OF NF-KB STIMULATED WITH NOSTOC SP. NO. 17   | 29 |
| FIGURE 16 RESPONSE RATIO OF NF-KB STIMULATED WITH NOSTOC MUSCORUM NO.30   | 30 |
| FIGURE 17 RESPONSE RATIO OF NF-KB STIMULATED WITH NOSTOC SP. NO.8   | 30 |
| FIGURE 18 RESPONSE RATIO OF IKB AFTER TREATMENT WITH NOSTOC SP. DE NO. 114.   | 31 |
| FIGURE 19 RESPONSE RATIO OF IKB AFTER TREATMENT WITH NOSTOC SP. NO. 17  | 32 |
| FIGURE 20 RESPONSE RATIO OF IKB AFTER TREATMENT WITH NOSTOC SP. NO.8  | 32 |
| FIGURE 21 ICAM-1 MEASUREMENTS OF UNKNOWN SAMPLE 7 AND SAMPLE 2  | 33 |
| FIGURE 22 ICAM-1 MEASUREMENT OF UNKNOWN SAMPLE 4 AND 5  | 34 |
| FIGURE 23 EVALUATION OF Z-FACTOR FOR THE ALPHALISA® IL-8 ASSAY  | 35 |
| FIGURE 24 KINETIC MEASUREMENT OF HTNF   | 35 |
| FIGURE 25 ALPHALISA DETECTED INHIBITION OF TNF STIMULATION WITH SB203580  | 36 |
| FIGURE 26 RESPONSIVENESS OF HLMVEC TO TNF IN ALPHALISA ASSAY  | 36 |
| FIGURE 27 ICAM-1 AND IL-8 EXPRESSION LEVEL OF NOSTOC SP. NO. 17   | 37 |
| FIGURE 28 ICAM-1 MEASUREMENT OF SEVERAL COMPOUNDS   | 38 |
| FIGURE 29 NUCLEAR TRANSLOCATION OF NFKB IN HUVEC CELLS  | 39 |
| FIGURE 30 TREATMENT OF ARTIFICIAL SKIN WITH SEVERAL SUBSTANCES  | 40 |

## Table of Contents

|   |      |
|---|------|
| Annotation  | II   |
| Acknowledgement   | IV   |
| List of relevant publications and author's contribution                   | V    |
| Abbreviations   | VIII |
| List of Figures   | X    |
| Table of Contents   | 0    |
| Introduction  | 1    |
| Screening for bioactive substances  | 1    |
| Inflammation and Cancer   | 2    |
| The NF- $\kappa$ B pathway  | 4    |
| Natural NF- $\kappa$ B inhibitors as anti-cancer agents                   | 6    |
| Novel cell-based assay methods  | 7    |
| AlphaLISA   | 7    |
| CellSensor <sup>®</sup> Cell-Based Pathway Analysis Assays                | 8    |
| Material  | 11   |
| Methods   | 14   |
| Alamar blue <sup>®</sup> Assay  | 14   |
| The Multitox-Fluor <sup>™</sup> Assay combined with the Caspase 3/7 Assay | 14   |
| ECIS Experiments  | 15   |
| LiveBlazer <sup>™</sup> Nf- $\kappa$ B Assay                              | 15   |
| LanthaScreen <sup>™</sup> I $\kappa$ B Assay                              | 16   |
| ICAM-1 ELISA  | 17   |
| AlphaLisa <sup>®</sup> Assay  | 18   |
| Stress fibres –microscopy   | 19   |
| NF $\kappa$ B nucleus translocation – microscopy                          | 19   |
| 3D Artificial skin model – wound healing                                  | 20   |
| Results   | 21   |
| Cytotoxicity Assays   | 21   |
| Alamar blue <sup>®</sup> Assay  | 21   |
| The Multitox-Fluor <sup>™</sup> Assay                                     | 24   |
| ECIS Experiment   | 27   |
| CellSensor <sup>®</sup> Cell-Based Pathway Analysis Assays                | 29   |
| LiveBlazer <sup>™</sup> Nf- $\kappa$ B Assay                              | 29   |
| LanthaScreen <sup>™</sup> I $\kappa$ B Assay                              | 31   |
| ICAM-1 Elisa  | 33   |
| AlphaLisa <sup>®</sup> Assay  | 34   |
| Nf- $\kappa$ B nucleus translocation                                      | 39   |
| 3D Artificial skin model – wound healing                                  | 40   |
| Discussion  | 41   |
| References  | 44   |
| Curriculum vitae  | 47   |

## **Introduction**

### **Screening for bioactive substances**

The systematic screening for bioactive substances began in the early 20<sup>th</sup> century and replaced the random drug discovery from nature. Beginning with the discovery of spongothymidine and spongouridine from the sponge *Tethya crypta*, found by Bergmann and Feeney (1951), which was leading to the synthesis of arabinosyl cytosine (Ara-C), an anti-cancer agent (1), the ocean was considered as a promising source of therapeutic agents because it harbors an enormous diversity of chemical compounds. Organisms like algae, fungi or bacteria produce secondary metabolites with an auspicious origin of therapeutically acting compounds. For example many anti-bacterial secondary metabolites have been found and they are used as antibiotics (e.g. penicillin, cephalosporines, streptomycin, and vancomycin), also a lot of anti-carcinogen substances are found (e.g. bleomycin, dactinomycin, doxorubicin and staurosporin) (2). Considering all anti-cancerogen drugs known from 1981 up to 2006 there are 100 new substances and 63% of them are natural derived compounds. Further there are 51 anti-inflammatory substances and 27% of them are natural derived (3). Regarding such data the screening of bioactive substances is an important second source of possible therapeutics in addition to the synthetic drugs of the combinatorial chemistry. Especially the Cyanobacteria produce a vast variety of secondary metabolites, due to their ability to exist even in extreme environments like in hot springs, in high salinity, in dry deserts or even in ice. Beside of these facts the Cyanobacteria have attracted the attention of researchers because a lot of strains produce toxins, which have harmful effects of animals and humans. Many of those toxins show also anti-bacterial, anti-fungal, antiviral or anti-tumor activities (4) (5) (6). Beginning with the late 80`s of the last century the cell-based assay methods became more important for the screening of bioactive substances. The benefit of these cell-based assays is the detailed information of the biological principles inside the cells (7) (8). Moreover for the requisition of scanning an immense amount of natural metabolites to discover several useful therapeutic agents, cell-based methods are fundamental to analyze the substances in defined and repeatable conditions.

## **Inflammation and Cancer**

Cancer is worldwide the leading cause of death, considering that 7.6 million people (13% of all deaths in 2008) die because of cancer (WHO Fact sheet N°297). The World Health Organization (WHO) estimates that this numbers will increase up to 11 million people worldwide till 2030. More than 30% of cancer could be prevented by avoiding the risk factors smoking, alcohol, low fruit and vegetable intake, physical inactivity and obesity (9) (10). Ten hallmarks of cancer are known (see Figure 1), enabling tumors to growth and to metastasize, first there is a continuous proliferation signaling, primary based on growth factors produced by the tumor themselves or stimulation of normal cells, aside the growth suppressors has to be downregulated by tumor suppressor genes. For continuous growth the tumor is enabling replicative immortality, therefore Telomerase, a DNA polymerase which adds telomere to the ends of telomeric DNA is expressed at significant levels in cancer cells. The tumor needs angiogenesis for transport of nutrients and oxygen therefore mainly the angiogenesis inducers VEGF and thrombospondin-1 are activated. Another hallmark is the activation of invasion and metastasis, several forms of invasions are known; for example the epithelial-mesenchymal transition (EMT) program transform epithelial cells so that they can invade and resist to apoptosis and they can disseminate. There is a amoeboid form of invasion as well as a collective form of invasion. Additional hallmark is deregulation of cellular energetics; meaning that cancer cells are able to reprogram their energy metabolism to “aerobic glycolysis” and upregulation of glucose transporter, in contrast to normal cells which process glucose to carbon dioxide in the mitochondria under aerobic conditions. A further hallmark is the avoiding of immune destruction of cancer cells, whose exact mechanism is still unknown yet as well as the genome instability and mutation by inactivating the components in the cell that are responsible for DNA maintenance because of mutations. Several years ago inflammation was considered as immune response to controvert tumors, but now tumor promoting inflammation is considered as important hallmark because of growth support due to growth factors, survival factors, proangiogenic factors and extracellular matrix modifying enzymes (11). Considering that if a hallmark of Cancer is inhibited tumor growth and progression should also be negatively affected. In Figure 1 examples for therapeutic agents are

described for the treatment of cancer grouped accordingly to their effects on one or more hallmark capabilities (11). Two inflammation pathways are identified, the intrinsic pathway where genetic events are causing inflammation and the extrinsic pathway with constant inflammation rising the risk or the progression of cancer. The central figure for cancer related inflammation are transcription factors like nuclear factor-kappaB (NF- $\kappa$ B), inflammatory cytokines like IL-6 and TNF $\alpha$  and signal transducer activator of transcription-3 (Stat3). The transcription factor NF- $\kappa$ B plays a key role in the tumor initiation and progression (12). Several factors can trigger inflammation, for example bacterias like *Helicobacter pylori*, viruses, environmental pollutions like cigarette smoke, stress or food ingredients like red meat. In the case of chronic inflammation there is, beside of other inflammation related diseases like diabetes, arthritis or Alzheimer, a high risk of tumor survival, proliferation and metastasis (13). Inflammation itself can destabilized the genome of cells, either by directly damage of the DNA or affecting the DNA repair system (12). Interestingly TNF has tumor necrotic effects at high dosis and tumor promoting effects at low dosis. For the extrinsic apoptotic pathway of TNF, TNF binds to the TNFR1 which is leading to the recruitment of **TNF receptor-associated protein with death domain** (TRADD) and **Fas-associated protein with death domain** (FADD) which then activates caspase 8 and caspase 3/7 followed by apoptosis (Figure 2) (14). There is also an intrinsic apoptotic pathway, activated by hypoxia, ischemia, reactive oxygen species or inhibition of growth factor signaling (15).

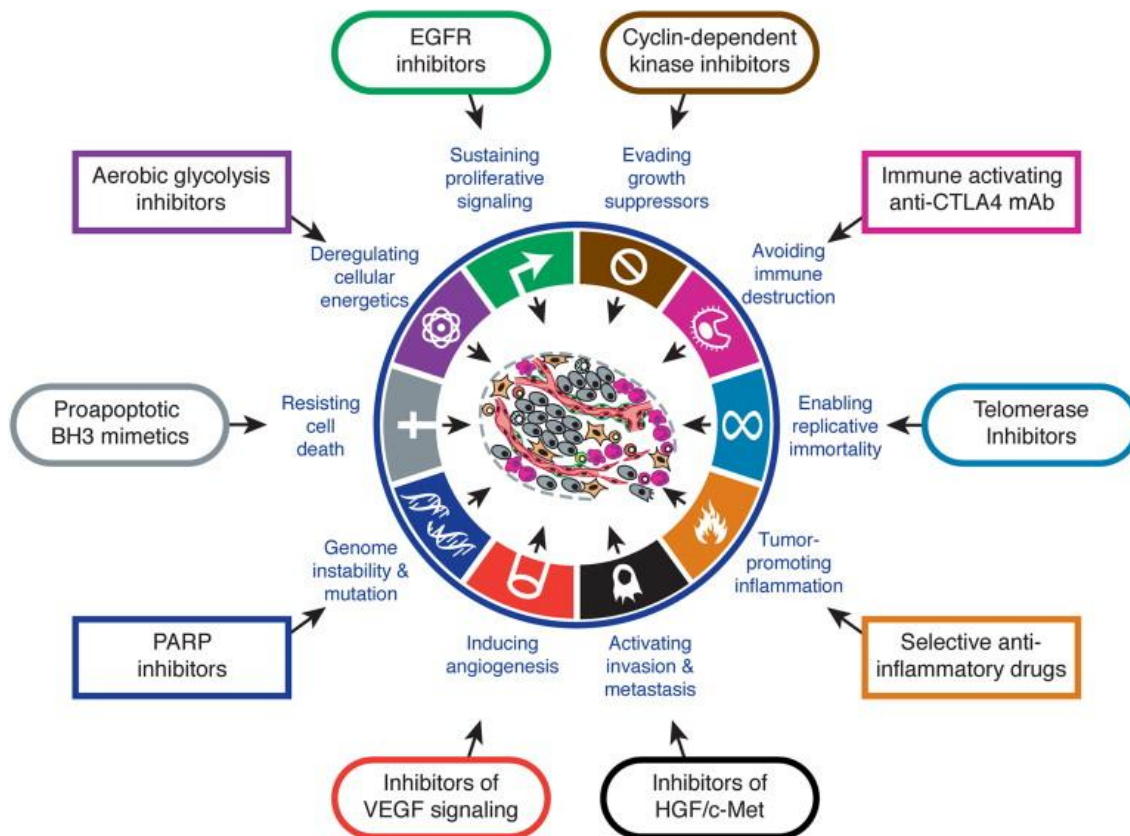


Figure 1 Hallmarks of Cancer with therapeutic targets (Figure taken from (11))

## The NF- $\kappa$ B pathway

NF- $\kappa$ B consists of five distinct subunits, p50, p52, c-Rel, RelA and RelB, they are structurally related and can form different combinations of homo- and heterodimers. The most common heterodimer is p50-RelA, also called NF- $\kappa$ B, this complex is retained in the cytoplasm and translocating into the nucleus to activate pro-inflammatory genes. The classical pathway TNF is binding to the TNFR2, followed by the recruitment of the TNFR associated factor (TRAF), receptor interacting protein (RIP), apoptosis signal-regulating kinase 1 (ASK1) and I $\kappa$ B kinase (IKK), a complex consisting of the subunits IKK $\alpha$ , IKK $\beta$  and a regulatory component IKK/NEMO. For TNF usually the subunit IKK $\beta$  phosphorylates I $\kappa$ B. The phosphorylation of I $\kappa$ B is leading to ubiquitination and degradation and NF- $\kappa$ B is translocated into the nucleus to activate genes, i.a. responsible for the production of pro-inflammatory cytokines. TNF can also mediate tumor angiogenesis by recruitment of Map/Erk kinase kinase (MEKK), the map kinase (MAPK) and the activator protein-1 (AP1) followed by inducing of pro-angiogenic factors like VEGF and IL-8 (Figure 2). The alternative pathway is resulting in the NF- $\kappa$ B heterodimer



p52-RelB, which is activated through the subunit IKK $\alpha$ . The alternative pathway can be activated through lymphotoxin  $\beta$  (or TNF $\beta$ ) or the B-cell activating factor (BAFF), a member of the TNF family produced by T cells and dendritic cells. The alternative pathway is phosphorylating the precursor relB/p100, leading to its cleavage into p52-RelB and translocation into the nucleus (14) (16) (17) (18) (19).

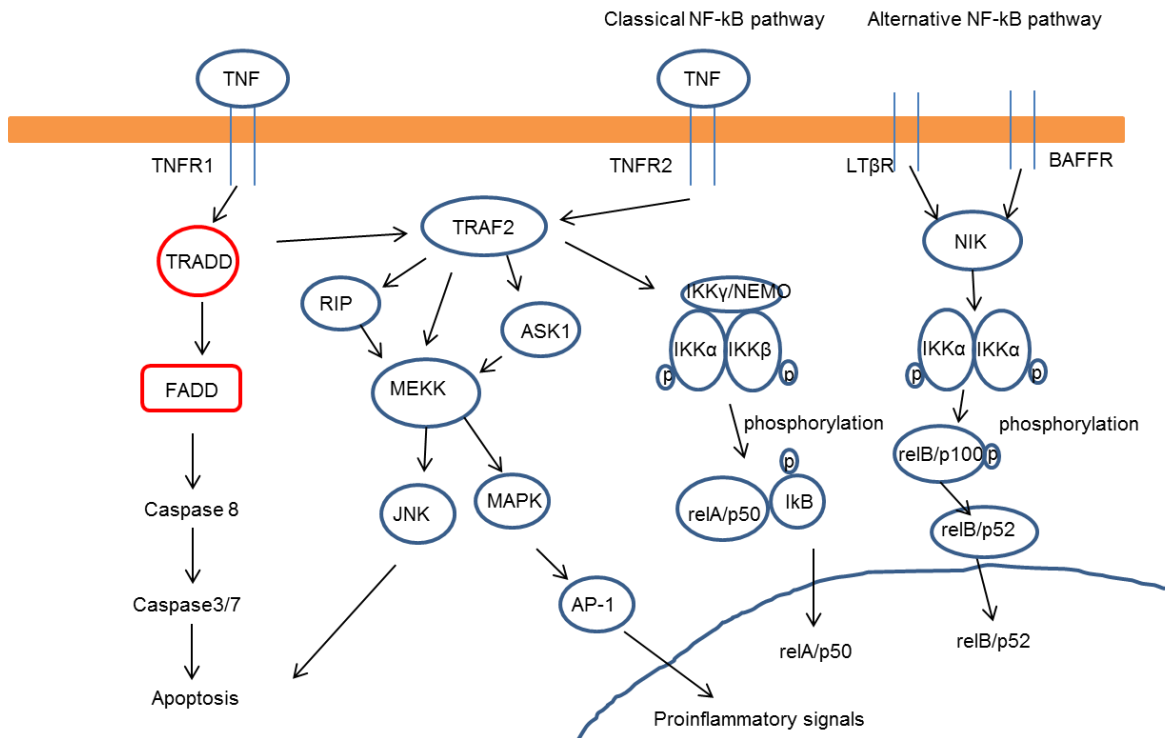


Figure 2 Tumor necrosis factor alpha pathway and the alternative NF- $\kappa$ B pathway

## **Natural NF- $\kappa$ B inhibitors as anti-cancer agents**

There are several oncogene viruses known, like the Epstein-Barr virus or the human T-cell leukemia virus type 1, to activate NF- $\kappa$ B. In many cancer cell lines the genes encoding for the subunits of NF- $\kappa$ B are found to be either overexpressed, amplified or rearranged. Moreover there are also gene alterations found encoding for the inhibitor I $\kappa$ B resulting in an inactivation of the function of I $\kappa$ B, for example in solid tumors of ovarian, colon or breast carcinomas or Melanomas (20). NF- $\kappa$ B inhibitors can affect different molecular targets; they can block NF- $\kappa$ B itself by binding of NF- $\kappa$ B to DNA or inhibit the proteasomal degradation of NF- $\kappa$ B. Another method is to inhibit the enzymes for the phosphorylation dependent polyubiquitination of I $\kappa$ B. The most important method is the inhibiting of IKK. Further NF- $\kappa$ B can be inhibited by antioxidants by reducing Reactive Oxygen Species (ROS) which can activate NF- $\kappa$ B otherwise (21). By analyzing natural substances isolated from plants which are used as folk medicine promising therapeutical agents are already found. An example for a natural NF- $\kappa$ B inhibitor is the substances Andrographolide, isolated from the plant *Andrographis* (*Andrographis paniculate*). Preincubation with Andrographolide decreased significantly the binding of NF- $\kappa$ B oligonucleotide to p50 (22). Another example is Curcumin, a component of Curry, showed in Melanoma cells with constantly overexpressed NF $\kappa$ B levels to down-regulated NF- $\kappa$ B and IKK activities (23). Marine natural products are also discovered as potent antimicrobial, anti-cancer, and anti-inflammatory compounds. An example therefore is the steroid IPL-576092 inspired by contignasterol (*Petrosia contignata*) which is in Phase II of the clinical trials for the treatment of cancer through NF- $\kappa$ B inhibition (24). Piceatannol, rank amongst stilbene and derived from red grapes is another example for an anti-inflammatory and anti-proliferative agent. Piceatannol suppresses the TNF induced NF- $\kappa$ B activation as well as the I $\kappa$ B $\alpha$  phosphorylation, p65 phosphorylation, and IKK activation (25).

## Novel cell-based assay methods

### AlphaLISA

Ullman and colleagues developed in 1994 the first bead based technique called LOCI (Luminescent Oxygen Channeling Immunoassay), this technology was then licensed by PerkinElmer Inc. for drug discovery applications in the year 1999 and marketed as AlphaScreen (Amplified Luminescent Proximity Homogeneous Assay) assay. The AlphaLISA technology was developed in 2006 for the automated screening of analytes in high throughput screening as an alternative for the classical ELISA technology. There are no time-consuming washing steps compared to the ELISA technology, this is a main advantage of the AlphaLISA technology because the washing steps require complex instrument programming for industrial automation and therefore increase assay costs and decrease precision. Furthermore the AlphaLISA assays are highly sensitive (sub-pM range) compared to the ELISA technology (pM range) as well as the decrease of the needed assay volume from 25-50  $\mu$ l to  $\geq 5$   $\mu$ l (26). The AlphaScreen assay is composed of two bead types, Donor beads and Acceptor beads, both are latex based, 250 nm diameters in size, and coated with hydrogel to minimize non-specific binding and self-aggregation. The small size of the beads has the advantage that they do not sediment in liquids and so they can be used for automated liquid handling. The beads are very stable in suspension, even at high temperatures, as well as in lyophilized form (27). There are streptavidin-coated Donor beads bound to a biotinylated antibody, they contain the photosensitizer phthalocyanine which reduce oxygen to its excited form singlet oxygen and Acceptor beads, also conjugated to an antibody contains thioxene. The singlet oxygen has a 4  $\mu$ sec half-life and can diffuse in this time approximately 200 nm in solution, if the singlet oxygen is near enough to an Acceptor bead the energy is transferred from the singlet oxygen to the thioxene which reacts with the singlet oxygen to a di-ketone derivative and emits light at 340 nm, in the AlphaScreen assay the emitted light of thioxene at 340 nm is submitted to anthracene and then to rubrene. The final compound in the cascade, rubrene, emits light at wavelengths of 520-620 nm. The Acceptor beads of the AlphaLISA assay contain a Europium chelate instead of anthracene and rubrene which emits light at 615 nm if it is excited

with 340 nm (Figure 3) (27). If there is no Acceptor bead the singlet oxygen falls to ground state and no signal is produced. The advantage of the AlphaLisa assay is that the Europium chelate is more intense and it's exactly spectral defined compared to broader AlphaScreen spectrum at 520-620 nm. The AlphaScreen assay is highly sensitive, each Donor bead can release up to 60,000 singlet oxygen molecules per second upon excitation at 680 nm resulting in a very high signal amplification. Moreover the AlphaScreen assay has low fluorescence backgrounds because of the time-resolved (20 msec) measurement and secondly because of the lower emission wavelength (615nm) compared to the higher excitation wavelength (680nm) which is the reason for most of the fluorescence background (27).

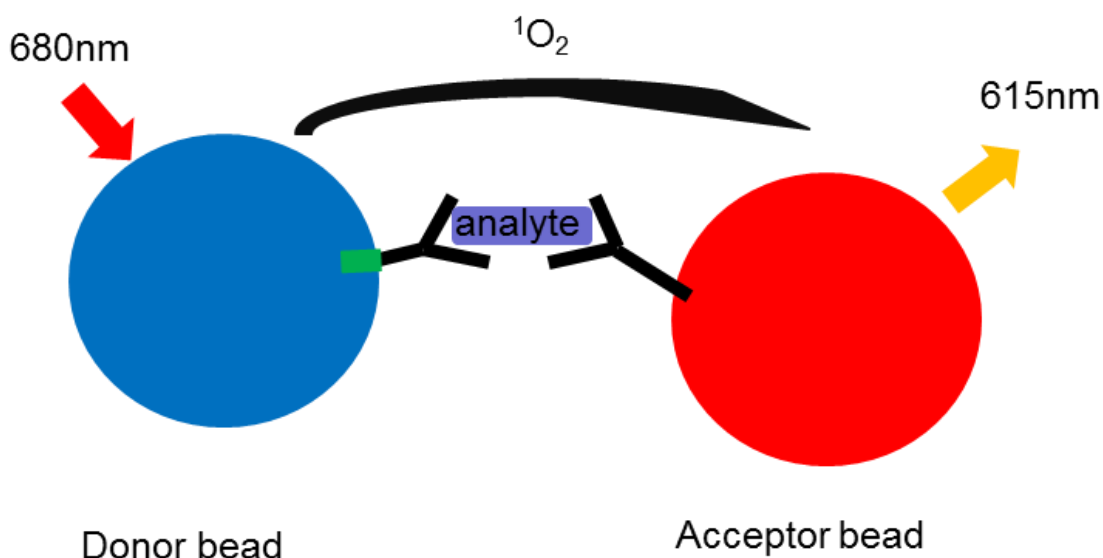


Figure 3 AlphaLISA technology

## CellSensor<sup>®</sup> Cell-Based Pathway Analysis Assays

### GeneBLAzer<sup>®</sup> technology

The basic principle of the GeneBLAzer<sup>®</sup> Technology is a Fluorescence Resonance Energy Transfer (FRET) substrate that generates a two-color (blue/green) readout of stimulated and unstimulated cells with minimal experimental background. This ratiometric method reduce the errors, e.g. cell number or substrat concentration, of an experimental procedure that can falsify the biological response. The CellSensor<sup>®</sup> reporter cell lines contain a stable integrated beta-lactamase reporter gene under control of the gene response element (NFkB, Anti-oxidant Response Element

(ARE)). The FRET-enabled substrate CCF4-AM (chloro-hydroxycoumarin fluorescein **AM** (acetoxymethyl)) lipophilic substrate enters the cell and is cleaved by cytoplasmic esterases to its negatively charged form which is retained in the cytosol. By illumination with 409 nm the substrate is emitting green light of 520 nm because of an energy transfer by FRET, if the substrate is cleaved by beta-lactamase the hydroxycoumarin part of the substrate is emitting blue light of 447 nm (Figure 4 ). Finally the coumarin : fluorescein ratio is calculated and this provides a normalized reporter response.

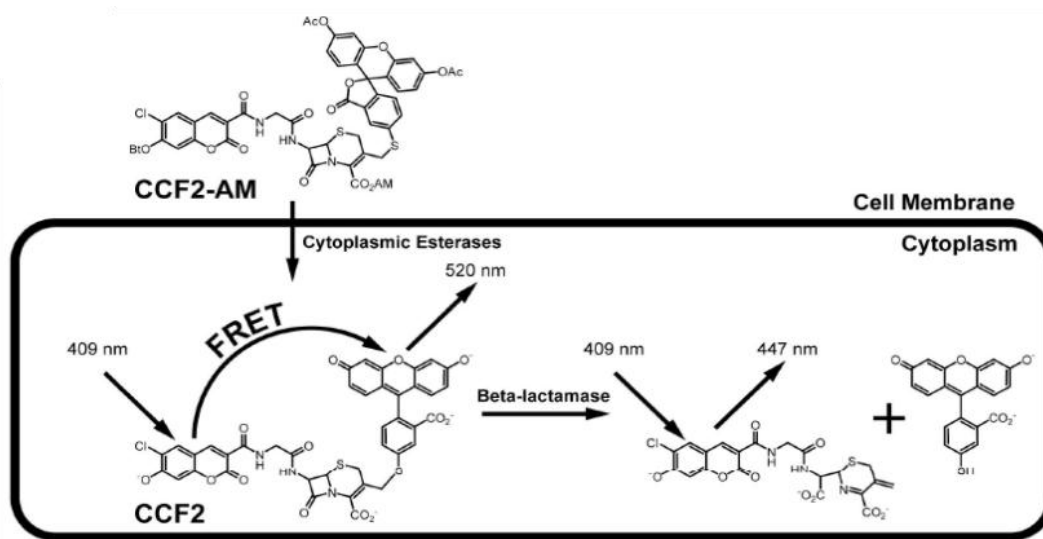


Figure 4 GeneBlazer® principle (Figure taken from (28))

## LanthaScreen® technology

The LanthaScreen® IκB alpha GripTite® cell line contains a stable integrated expression vector encoding for a GFP fusion protein (GFP is fused to the N-terminus of IκB alpha) under the control of a CMV (cytomegalovirus) promoter stably transfected into a modified human kidney HEK293 GripTite® cells. HEK293 cells showing inducible activation of the NFκB pathway, this cell line allows therefore the analysis of IKK activity using GFP-IκB alpha phosphorylation as readout. The principle is based on the **T**ime-**R**esolved **F**luorescence **R**esonance **E**nergy **T**ransfer (TR-FRET), therefore a terbium (Tb<sup>3+</sup>) labeled phosphospecific antibody binds GFP, a suitable TR-FRET acceptor for the excited-state Tb fluorophore, resulting in an increase in the TR-FRET signal (Figure 5). The terbium fluorophore has an extended excited-state life time in the range of milliseconds (time-resolved) compared to the majority of fluorophores which possess excited-state lifetimes on the order of nanoseconds.

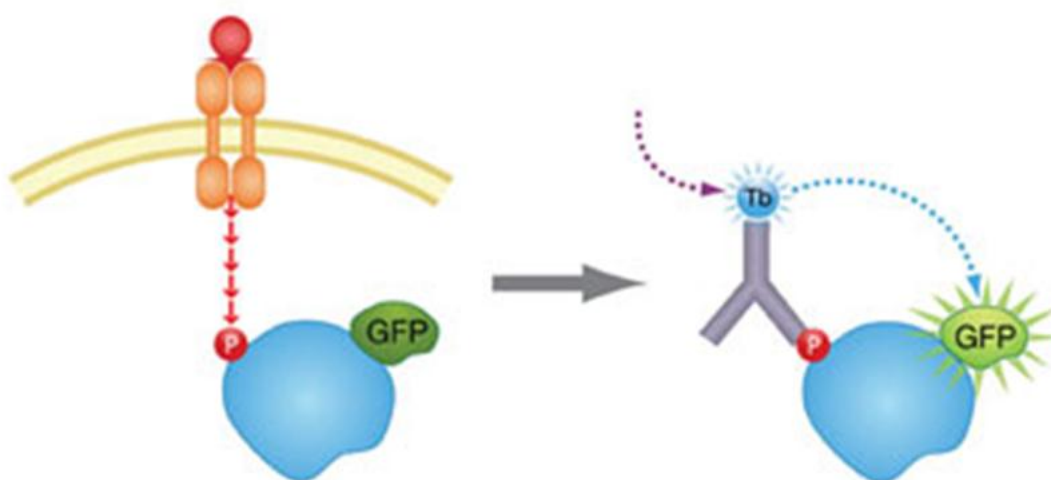


Figure 5 LanthaScreen® principle (Figure taken from (29))

## Material

### Biological material

- CellSensor® NFκB-*bla* FreeStyle™ 293F Cell Line (LifeTech, K1663)
- CellSensor™ ARE-*bla* Hep G2 cell line (LifeTech, K1208)
- HaCaT (gift from AKH Vienna)
- HLMVEC (Provitro, 1210144)
- HUVEC GFP (gift from AKH Vienna)
- LanthaScreen™ IκB alpha GripTite cell line (LifeTech, K1489)
- NIH-3T3 fibroblasts (ATCC, CRL-1658™)
- Primary Huvec (Provitro, 121 0111)

### Chemicals and kits

- Actinomycin D (LifeTech, PHZ1024)
- Alamar blue (LifeTech, VXDAL1025)
- AlphaLisa ICAM 1 kit (PerkinElmer, Inc., AL282C)
- AlphaLisa IL-8 kit (PerkinElmer, Inc., AL224)
- AlphaLISA® ICAM-1 Immunoassay Research kit (Perkin Elmer, AL282C)
- AlphaLISA® IL-8 Immunoassay Research kit (Perkin Elmer, AL224C)
- BD Matrigel Basement Membrane Matix (VWR, 734-1100)
- Blastocidin S (Invivogen, ant-bl-1)
- Bovine Serum Albumin Standard (Pierce, 10381314)
- Caspase 3/7 Glo (Promega, G8091)
- Charcoal stripped FBS (LifeTech, 12676-011)
- Collagen 1 (LifeTech, A1048301)
- Digitonin (Sigma, D141-100MG)
- Dimethylsulfoxide (Sigma, D5879-100ml)
- DMEM (LifeTech, 11960044 )
- Endothelial medium (PAA, U15-002)
- ER-Tracker™ Green (LifeTech, E34251)
- ER-Tracker™ Red (LifeTech, E34250)
- Fetal Bovine Serum (LifeTech, 10270106)

- Fetal Bovine Serum dialyzed (LifeTech, 26400-044)
- Attophos Fluorescent Substrate System (Promega, S1000)
- Diethanolamine (Sigma, 31589)
- Fibronectin (Sigma, F2006-1MG)
- Formaldehyde (Carl-Roth, F1635-500ML)
- GIBCO® FreeStyle™ 293 Expression Medium (LifeTech, 12338-018)
- goat-anti-mouse IgG-alkaline phosphatase (Sigma, A3562-.25ML)
- HEPES buffer solution (Sigma, 83264)
- Hoechst 33342 (Lonza, PA-3014)
- IgG from murine serum (Sigma, I5381-1MG)
- LanthaScreen™ Cellular Assay Lysis Buffer (LifeTech, PV5598)
- L-Glutamin (LifeTech, 25030024)
- LiveBlazer Fret B/G loading kit (LifeTech, K1095)
- Mouse-anti-human ICAM-1 mAb (Sigma, WH0003383M1)
- MOWIOL® 4-88 (Merck, 475904)
- MultiTox-Fluor Multiplex Cytotoxicity Assay (Promega, G9201)
- NaOH (Merck, 1.06469.1000)
- Nf-κB inhibitor SB203580 (Sigma, S8307-1MG)
- Nonessential amino acids (NEAA) (LifeTech, 11140-050)
- Opti-MEM (LifeTech, 11058-021)
- Penicillin/Streptomycin (LifeTech, 15140122)
- Phalloidin Alexa Fluor 568 (LifeTech, A12380)
- Phosphatase inhibitor mix (Sigma, P2850-1ML)
- Phosphate Buffered Saline (LifeTech, 10010056)
- Protease inhibitor mix (Sigma, P8340-1ML)
- RPMI 1640 (LifeTech, 31870074)
- RPMI 1640 Phenol red free (LifeTech, 32404-014)
- SB203580 (Sigma, S8307-1MG)
- Sodium pyruvate (LifeTech, S8636)
- Tert-butylhydroquinone (Sigma, 112941-5G)
- Triton X-100 (Sigma, 93443-100ML)



- Trypsin 0.25% (LifeTech, 25200-056)
- Tumour Necrosis Factor alpha (NIBSC, 88/786)
- UltraPure™ DNase/RNase-Free Distilled Water (LifeTech, 10977-049)

### **Consumables**

- 96well ECIS plates with 10 electrodes (Applied Biophysics, 96W10E+)
- Microplates 96w, black, transparent bottom (Nunc, 165305)
- Microplates 96w, cell grade plus, black, transparent bottom (Brand, 7624490)
- Microplates 96w, cell grade plus, white (Brand, 4.000333)
- Microplates 96w, transparent (Nunc, 167008)
- Microplate 384w, black, transparent bottom (Brand, 781981)
- Oris Cell Migration Assay Kit (amsbio, CMA5.101)
- Permanox Chamber slides 16 wells (Nunc, 178599)

### **Equipment**

- AlphaScreen Cartridge (Molecular devices, A6847)
- Confocal Laser Scanning Microscope (Leika, TCS SP2)
- ECISz instrument (Applied Biophysics)
- FL GBlazer Cartridge (Molecular devices, A41577)
- SpectraMax Paradigm Multi-Mode Microplate Detection Platform (Molecular devices, Inc.)

## Methods

### Alamar blue<sup>®</sup> Assay

HLMVEC cells were seeded in a concentration of 20000 cells per well in a black 96 well plate (Brand cell grade) with transparent bottom in 90 µl RPMI medium and incubated for 4-6 h at 37°C and 5% CO<sub>2</sub>. The cells were treated with the test compounds in triplicates and 6 wells were left out for the controls. After 17 h in three wells 1% Triton-X was added as negative control for 1 h the other three wells were left as positive control. After addition of Alamar blue<sup>®</sup> solution (1% final concentration) the plate was incubated for at least 3 hours at 37 °C and 5% CO<sub>2</sub>, then the plate was read in the Paradigm Detection Platform at an excitation wavelength of 535 nm, and an emission wavelength of 595 nm. The percentage of living cells was calculated using the following formula:

$$\frac{([\text{test signal}] - [\text{negative control value}]) \times 100}{([\text{positive control value}] - [\text{negative control value}])}$$

### The Multitox-Fluor<sup>™</sup> Assay combined with the Caspase 3/7 Assay

The GF-AFC live-cell and the AAF-R110 dead-cell substrates were added to the assay buffer. The HLMVEC were plated in a concentration of 20000 cells per well in 50 µl endothelial medium in a transparent 96 well plate, the test substances were added and the plate was incubated for 4-6 h in the incubator at 37 °C. Three wells were left untreated as a positive control and a standard curve with hTNF starting from 10 ng.ml<sup>-1</sup>, 1 ng/ml, 0.4 ng.ml<sup>-1</sup> and 0.01 ng.ml<sup>-1</sup> was added. For the negative control 30 µg.ml<sup>-1</sup> Digitonin was used. After incubation the Multitox-Fluor<sup>™</sup> Reagent was added to the wells (50% final concentration) and incubated at 37 °C for 1 h in the dark. The fluorescence was measured at Ex 406 nm and Em 465 nm (live-cells), Em 542 nm (dead-cells). The mean of each emission was calculated and the percentage of living cells compared to the untreated control was determined with the following formula:

$$\frac{([\text{test signal}] - [\text{negative control value}]) \times 100}{([\text{positive control value}] - [\text{negative control value}]}$$

The percentage of dead cells was calculated from the dead-cell emission Em 542 nm using the formula: 100% - mean Em 542 nm. For the Caspase 3/7 Assay the Caspase-Glo Substrate was added to the Caspase-Glo Buffer and this was added to a final concentration of 50% to all wells. The plate was incubated for 30-60 min in the dark, then the luminescence was measured.

## **ECIS Experiments**

A 96 well ECIS plate with 10 electrodes per well was taken and pre-incubated with fibronectin (1  $\mu\text{g.ml}^{-1}$ ) for at least 1 h. Then 60 000 HLMVEC were plated per well in 200  $\mu\text{l}$  Endothelial cell medium (1% Pen/Strep, 10% FBS) and incubated overnight. On the next day the medium was changed and 200  $\mu\text{l}$  Endothelial cell medium (1% Pen/Strep, 0% FBS) was used and the cells were stimulated with the test substances or the positive control Triton-X100 in sextuples and measured with an AC of 4000 Hz.

## **LiveBlazer™ Nf- $\kappa$ B Assay**

The CellSensor® NF- $\kappa$ B-bla Hek293 cells were plated at a concentration of 40000 cells/well in 50  $\mu\text{l}$  FreeStyle medium (1% Pen/Strep, 2% FBS dialyzed) in triplicates overnight. The test substances were added for 30 min, and then hTNF (final concentration 4  $\text{ng.ml}^{-1}$ ) was added. For the background control three wells were left only with medium. A standard curve started at a concentration of 0.01  $\text{ng.ml}^{-1}$ , 0.1  $\text{ng.ml}^{-1}$ , 0.4  $\text{ng.ml}^{-1}$ , 1  $\text{ng.ml}^{-1}$  and 10  $\text{ng.ml}^{-1}$  hTNF. The microplate was incubated at 37 °C for 4 h. The LiveBlazer™ Substrate loading solution (6 x) was prepared as follows:

1. 60  $\mu\text{l}$  of solution B is mixed with 6  $\mu\text{l}$  of the CCF4-Am substrate, vortex
2. add 934  $\mu\text{l}$  of solution C, vortex

10  $\mu\text{l}$  of this mixture was added per well and incubated in the dark at room temperature. The microplate was measured in the Paradigm Detection Reader

(FRET-fluorescence bottom measurement, Ex 406 nm, Em 465 nm, Em 535 nm).

Calculate the results as follows:

1. Calculate the mean of the cell free control from Em 465 nm and Em 535 nm
2. Subtract the mean from Em 465 nm and Em 535 nm
3. Emission Ratio = Em 465 nm / Em 535 nm
4. Mean of the unstimulated Emission Ratio control
5. Response Ratio = Emission Ratio / mean unstimulated Emission Ratio

### **LanthaScreen™ IκB Assay**

LanthaScreen™ IκB alpha GripTite™ cells were plated in a concentration of 40000 cells/well in 50 μl Assay Medium (Optimem with 1% Charcoal stripped FBS, 0.1 mM NEAA, 1 mM Sodium pyruvate, 1% Pen/Strep) into a white 96 well plate and incubated overnight. On the next day the cells were stimulated with the test samples 30 min before addition of hTNF (0.4 ng.ml<sup>-1</sup>). An hTNF standard curve starting from 0.01 ng.ml<sup>-1</sup>, 0.1 ng.ml<sup>-1</sup>, 0.4 ng.ml<sup>-1</sup>, 1 ng.ml<sup>-1</sup> up to 10 ng.ml<sup>-1</sup> was added. The plate was incubated at 37 °C and 5 % CO<sub>2</sub> for 30 min. The media was suck from each well and 30 μl lysis buffer (inclusion of protease inhibitor 1/100 diluted, phosphatase inhibitor 1/100 diluted and the terbium labeled antibody 2 nM) was added, in three wells a negative control without cells just with lysis buffer was added. The plate was incubated 1h at room temperature in the dark. Then the plate was measured using TR-FRET bottom read at an excitation of Ex 360 nm, the first emission at Em 465 nm and the second emission at Em 535 nm. The result was calculated as follows:

1. Mean of the negative control at Em 465 nm and Em 535 nm
2. Subtract this mean from the values of Em 465 nm and Em 535 nm
3. Emission Ratio = 535 nm / 465 nm
4. Calculate mean of the negative Emission Ratio control
5. Subtract this mean from the Emission Ratio

## ICAM-1 ELISA

HLMVEC were plated in 100  $\mu$ l Endothelial medium at a concentration of 20000 cells/well in a flat-bottomed 96 well plate. The plate was incubated for 4-6 h at 37 °C incubator. The cells were pre-incubated for 30 min with the test substances, which were then stimulated with 10 ng.ml<sup>-1</sup> TNF. As positive control hTNF (0.1, 1, 10 ng.ml<sup>-1</sup>) was used. Three wells were left for control basal expression and 3 wells were left for the control antibody signal.

1. after 18 h incubation, the cells were centrifuged at 1500 rpm for 10 min. Then the medium was removed and the plate was washed with sterile PBS, 1x5 min, 200  $\mu$ l per well, shaker (level 700)
2. The PBS was removed and 50  $\mu$ l per well of -20°C methanol was added, the plate was put at -20 °C for 2 min.
3. the plate was washed 3 x with sterile PBS, 200  $\mu$ l per well, shaker (level 700)
4. 200  $\mu$ l of 5% BSA solution was added to each well in order to block aspecific binding, 45 min, RT; no shaking
5. 1<sup>st</sup> Antibody mouse anti-human ICAM-1 IgG, diluted in PBS + 5% BSA, 1:2000, 30  $\mu$ l per well, 45 min, RT; smooth shaking (level 600), also in 3 wells of the control (**basal ICAM-1 value**). No anti-ICAM-1 antibody was added in the 3 wells for the control antibody signal, murine IgG (**ctrl Ab signal**), also at a 1:2000 dilution will be added instead. In the latter wells, 30  $\mu$ l per well PBS + 5% BSA will be added instead.
6. the plate was washed with 200  $\mu$ l PBS/5% BSA, 2 x 5 min, shaker (level 700)
7. 2<sup>nd</sup> Antibody (Rabbit-anti-mouse IgG-alkaline phosphatase) diluted in PBS + 5% BSA was added, 1:300 from stock solution, 50  $\mu$ l per well, 60 min, RT; smooth shaking (level 600) to all wells

8. plate was washed 2 x 5min with PBS/BSA and 1 x with 2.5 M Diethanolamin buffer, pH 9.5, 1 x 5 min, 200 µl per well, shaker (level 700)
9. 100 µl per well of the Attophos substrate was added to each well then the reaction was measured from 2 min on at excitation wavelength 485 nm and emission wavelength 530 nm in the Multimode detector.

### **Data Processing**

The ICAM-1 (%) expression level is calculated as follows:

$$\frac{([\text{test signal}] - [\text{ctrl Ab signal}]) \times 100\%}{([\text{basal ICAM-1 value}] - [\text{ctrl Ab signal}])}$$

### **AlphaLisa<sup>®</sup> Assay**

20000 HLMVEC per well were seeded into a white, transparent bottom, 96 well plate in 100 µl Endothelial medium and incubated for 4-6 hours. The cells were treated with hTNF international standard (0.001 ng.ml<sup>-1</sup>, 0.01 ng.ml<sup>-1</sup>, 0.1 ng.ml<sup>-1</sup> and 1 ng.ml<sup>-1</sup>), the test substances were pre-incubated for 30 min, and then 0.4 ng.ml<sup>-1</sup> hTNF was added. Three wells were left untreated as a negative control. After 18 h the supernatant was suck (stored at 4 °C for the AlphaLisa<sup>®</sup> IL-8 Assay) and the biotinylated antibody (1 nM final concentration), mixed with the AlphaLisa<sup>®</sup> anti-ICAM-1 Acceptor Beads (10 µg.ml<sup>-1</sup> final concentration) was added on the cells in the wells. The plate was incubated at room temperature for 1 h. Then the Streptavidin-coated Donor Bead solution was added (40 µg.ml<sup>-1</sup> final concentration) and the plate was incubated in the dark at room temperature for another 30 min. After incubation at room temperature in the dark for 30 min the plate was measured with the Paradigm detection reader at an excitation of Ex 680 nm and an emission of Em 570 nm (fluorescence top read). The mean of the measured values were calculated and the percentage of the ICAM 1 or IL-8 upregulation compared to the unstimulated control was determined.

For the measurement of the IL-8 level the supernatant was taken from the AlphaLisa® ICAM-1 Assay and mixed with the biotinylated anti-IL-8 antibody (1nM final concentration) and the AlphaLisa® anti-ICAM-1 Acceptor Beads (10  $\mu\text{g}\cdot\text{ml}^{-1}$  final concentration) into a white, transparent bottom, 96 well plate. The experiment was finalized in the same way like the AlphaLisa ICAM-1 assay.

### **Stress fibres –microscopy**

Primary Huvec cells are plated on a fibronectin (1  $\mu\text{g}/\text{ml}$ ) 1h pre-coated 16 well permanox chamber slide at a concentration of 50000 cells per well in 200  $\mu\text{l}$  Endothelial medium overnight. The next day the cells are pre-stimulated 30 min with the test substances or the Nf- $\kappa\text{B}$  inhibitor Parthenolide, then add TNF in a concentration of 10  $\text{ng}\cdot\text{ml}^{-1}$ . For the controls 1-2 wells left untreated and 1-2 wells are treated with TNF (10  $\text{ng}\cdot\text{ml}^{-1}$ ) only. The slide is fixed in 4% Formaldehyde (10 min), washed 1 x and then treated with a 0.1 % Triton-X100 solution for 20 min. The cells are washed with PBS 2 x, then add Phalloidin Alexa Fluor 568 in a concentration of 125  $\mu\text{g}/\text{ml}$  for 1h. At the end of the incubation time the cells were treated with Hoechst 33342 (10  $\mu\text{g}\cdot\text{ml}^{-1}$ ) for 10 min. The cells are washed 3 x and betted in Mowiol®.

### **NF $\kappa\text{B}$ nucleus translocation – microscopy**

Primary Huvec cell were seeded at a concentration of 40000 cells per well in a fibronectin (1  $\mu\text{g}\cdot\text{ml}^{-1}$ ) pre-coated 16 well permanox chamber slide and incubated overnight. The next day the cell were stimulated with hTNF (final concentrations 10, 1, 0.1  $\text{ng}\cdot\text{ml}^{-1}$ ) as positive controls. Cyanobacterial fractions (final concentrations 100, 10, 1  $\mu\text{g}\cdot\text{ml}^{-1}$ ) were taken and pre-incubated for 30 min, then stimulated with 0.1  $\text{ng}\cdot\text{ml}^{-1}$  hTNF for 1 h. As negative control the Nf- $\kappa\text{B}$  inhibitor SB203580 (final concentration 100  $\mu\text{M}$ ) was taken, pre-incubated for 30 min, then stimulated with 0.1  $\text{ng}\cdot\text{ml}^{-1}$  hTNF.

### 3D Artificial skin model – wound healing

Prepare the Collagen Solution like in the manual described: Therefore prepare a 3 mg/ml Collagen Solution, calculate the amount of the 10 x PBS, 1N NaOH and dH<sub>2</sub>O needed:

Volume of collagen needed (**V1**) = Final conc. of collagen x Total Volume (V) / Initial conc. of collagen

Volume of 10X PBS needed (**V2**) = Total Volume (V) / 10

Volume of 1N NaOH needed (**V3**) = Final volume of collagen needed (V1) x 0.025

Volume of dH<sub>2</sub>O needed (**V4**) = Total Volume (V) - (V1 + V2 + V3)

To prevent gelation do all the steps with pre-cooled reagents on ice.

Stable transfected NIH-3T3 fibroblasts (blue) and Huvec GFP were plated at a concentration of 70000 cells per well in 70 µl per well Collagen Solution for 45 min in the incubator, then add 100 µl medium and incubate it overnight. After 24 h the stable transfected HaCaT keratinocytes (red) (30000 per well) were plated on top of the collagen 1 - fibroblasts mixture. On the next day remove the Oris™ Stoppers with the metal stopper removal tool; then remove the medium with a pipette using the Oris™ Migration Mask under the 96 well plate.

Mix the test substances with the Collagen Solution and pipette 10 µl in the exclusion zone. Wait 10 min before the addition of 200 µl medium. After 0 h and 6 h measure the 96 well plate with the Oris™ Migration Mask in a detection reader (fluorescence bottom read, Em 485 nm, Ex 535 nm).



## Results

### Cytotoxicity Assays

#### Alamar blue® Assay

The Alamar blue® Assay measures the metabolic activity of the hole cells. The result in (Figure 6) shows the cell viability after 18 h of exposure of HLMVEC with several crude extracts of cyanobacteria (Nostoc). The substances N15 and N28 are to 90% toxic for the 1/10 dilution. Substances N27 is to 50% toxic for HLMVEC for the 1/10 dilution. In this experiment just substances N17 had no toxic effect to the cells.

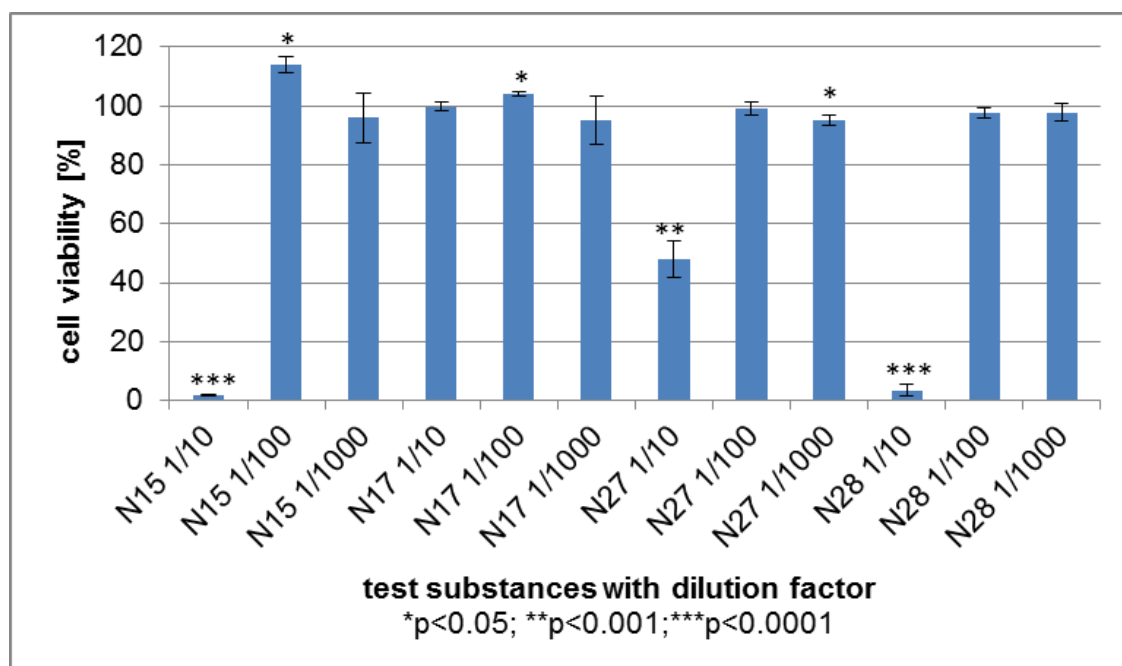


Figure 6 Evaluation of the cytotoxicity of several cyanobacterial compounds

Beside of crude extracts also purified compounds are tested in our experiments. Figure 7 shows the cytotoxicity of Nostoc sp. De No.114 Fractions m/z 781.8, m/z 875.7 and 699.7 + 694.2 show a cell viability of approximately 60% and fractions m/z 1012.9, m/z 803.7 + 823.8 + 805.9 + 823.8 and m/z 789.8 + 807.8 show a reduced cell viability of approximately 80%. The fractions m/z 537.5, m/z 821.7 + 847.8 and 789.8 + 807.8 showed no significant cytotoxicity in this experiment.

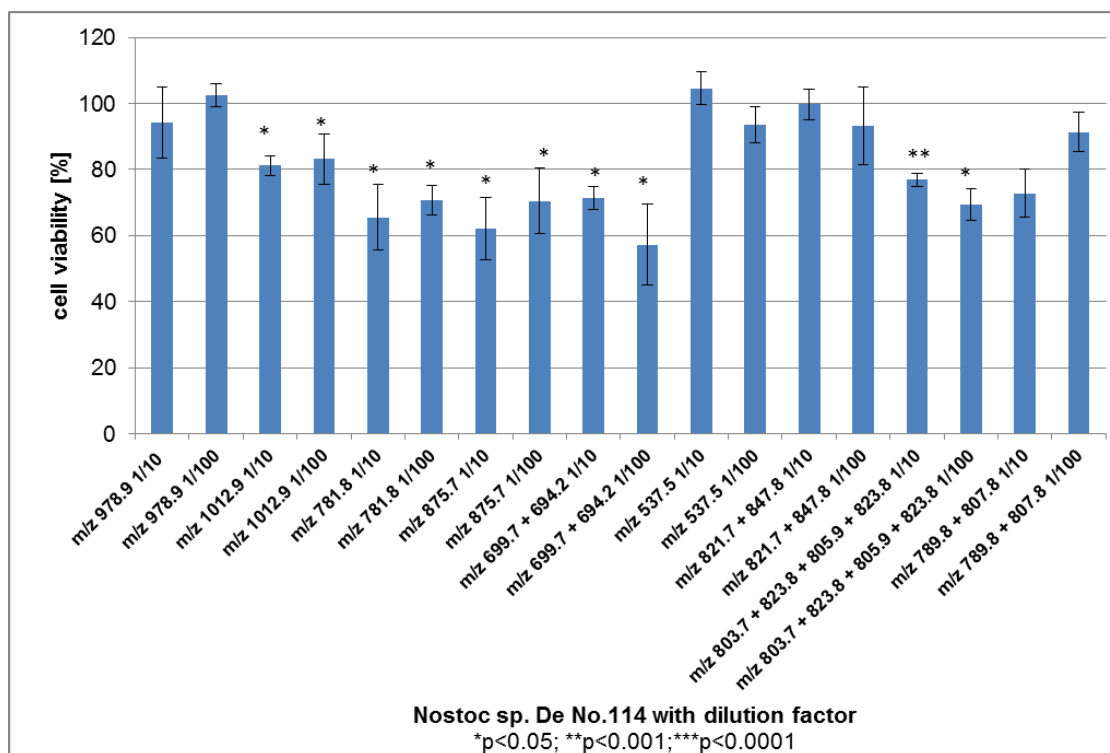


Figure 7 Cytotoxicity measurement of Nostoc sp. De No.114

In Figure 8 the cytotoxicity measurement of some fractions of Nostoc sp. No.17, Calu1533 No.183 and Nostoc muscorum No.30 are shown. There is no significant cytotoxicity of Nostoc sp. No.17 m/z 1184.5, Nostoc sp. No.8 m/z 721.6 and Calu1533 No.183 m/z 449 fractions for the concentrations 10 ng.ml<sup>-1</sup> and 1 ng.ml<sup>-1</sup>. Nostoc muscorum No. 30 m/z 744 (1 ng.ml<sup>-1</sup>), Nostoc muscorum No. 30 fractions m/z 815, 880, 781, 777 (concentration 10 ng.ml<sup>-1</sup>) and Nostoc muscorum No. 30 F5 (1/2 dilution) as well as Nostoc sp. No.17 m/z 1081.4 (concentration 10 ng.ml<sup>-1</sup>) show a significant toxicity of 10-20%.

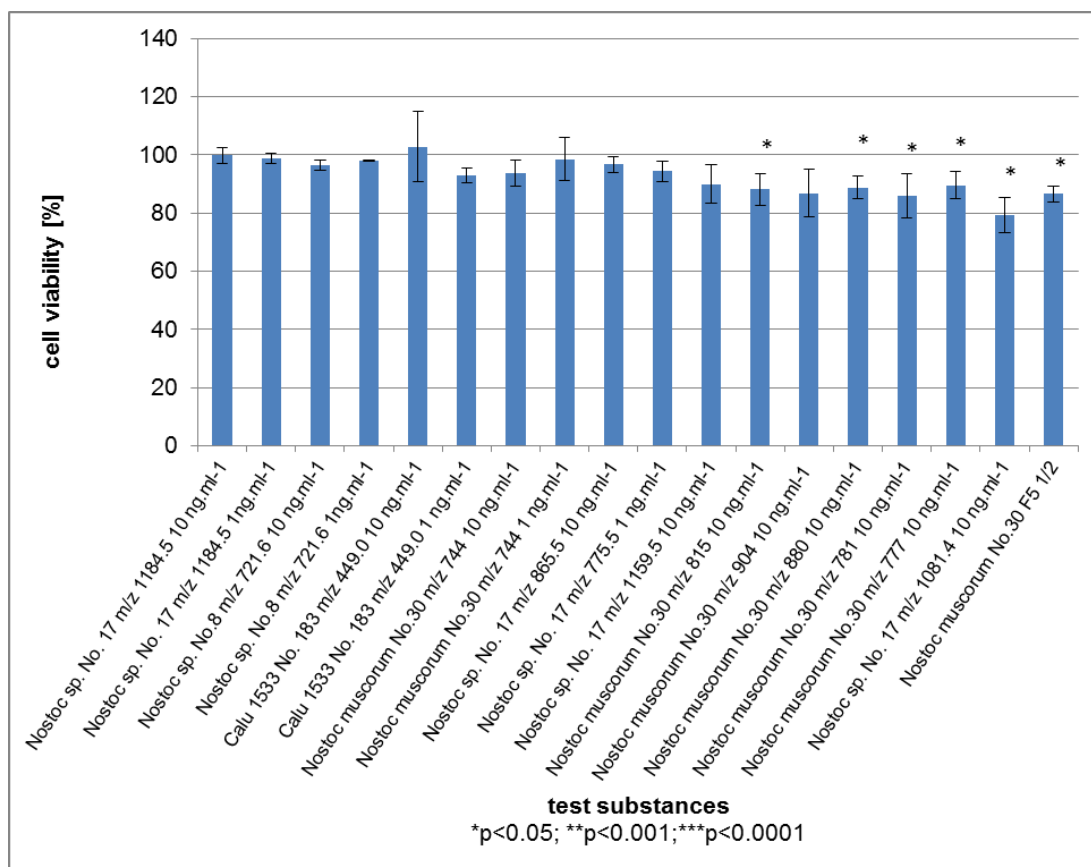


Figure 8 Cytotoxicity measurement of Nostoc sp. No.17 and No.8, Calu1533 No.183 and Nostoc muscorum No.30

Figure 9 shows the Cytotoxicity of Nostoc strain No.8, in this experiment the fractions m/z 1111.8 is significant toxic for the cells, fraction m/z 899.7 is 30% toxic for the 1/10 dilution and fractions m/z 1133.8 + 1219.8 and 1119.8 are significant toxic. Fraction m/z 1119.9 is to 90% toxic for the 1/10 dilution decreasing with rising dilution factors.

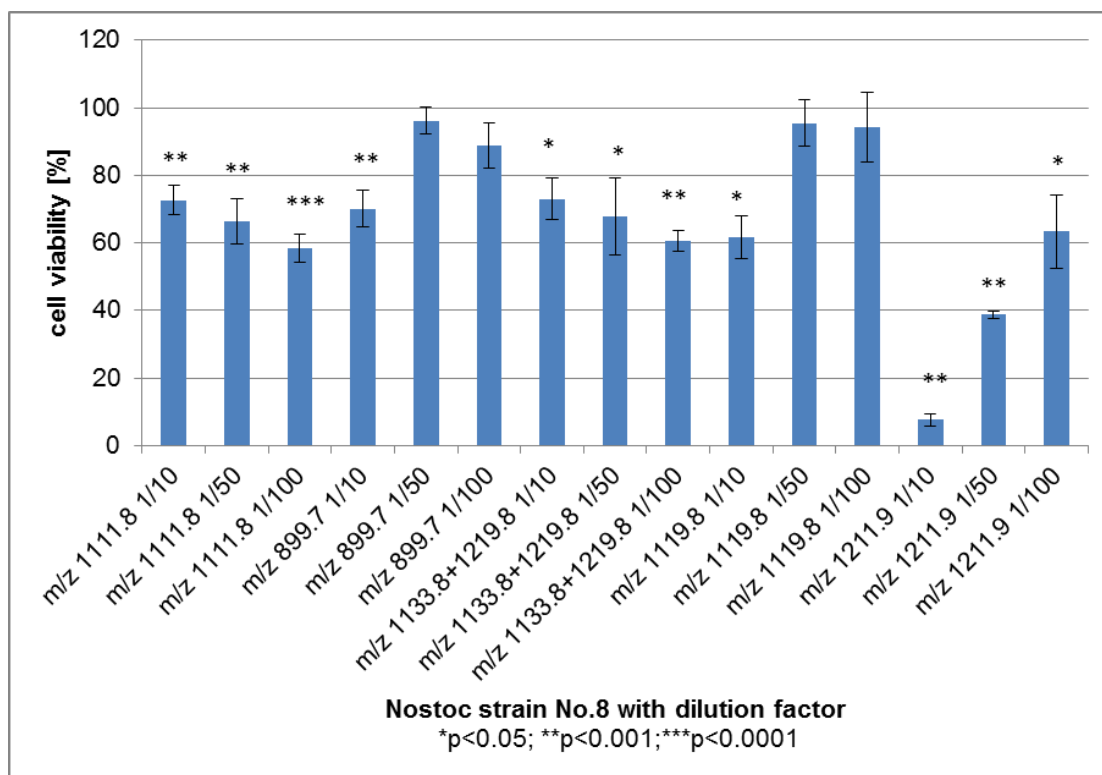
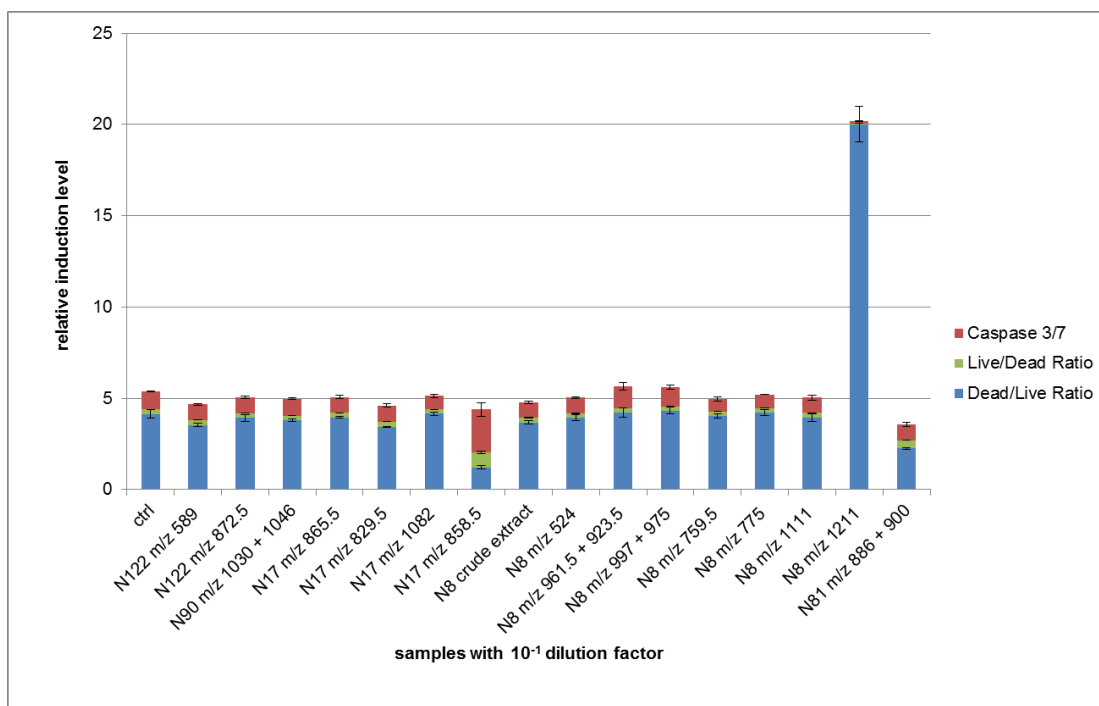


Figure 9 Cytotoxicity measurement of Nostoc strain No.8

### The Multitox-Fluor™ Assay

The Multitox-Fluor™ Assay is a method to measure the viable and the dead cells at the same time, in this experiment we combined this with an Caspase 3/7 Assay.

The samples we used for this experiment were several fractions of a pure extract of a cyanobacterial compounds (Nostoc). We saw a high cytotoxicity of the Nostoc strain No.8 with the mass of m/z 1211 with a viability of  $52.9\% \pm 2.4\%$  and a caspase 3/7 downregulation to  $11.4\% \pm 2.9\%$  whereas the Nostoc strain N17 m/z 858.5 shows a high cell viability of  $219.3\% \pm 6.7\%$  combined with a caspase 3/7 activity of  $236.2\% \pm 15.7\%$  (Figure 10).



**Figure 10** Cyanobacterial compounds (Nostoc) were tested for cytotoxicity and multiplexed to detect apoptosis induction.

In Figure 11 we measured the viability and the toxicity for the Nostoc sp. N122 m/z 589 and m/z 872.5 for the dilution factors from 1/10 up to 1/640. The fraction m/z 872.5 the 1/10 dilution showed a viability of 170%  $\pm$  11.6% which is decreasing to 97.5%  $\pm$  5.7% for the 1/640 dilution. For the fraction m/z 589 a viability of 83.6%  $\pm$  5.7% for the 1/10 dilution was measured increasing to 118.9%  $\pm$  9.1% for the 1/640 dilution. As control we used Triton X-100 in a 0.1% dilution which reduced the viability to 24.8%  $\pm$  2.0%.

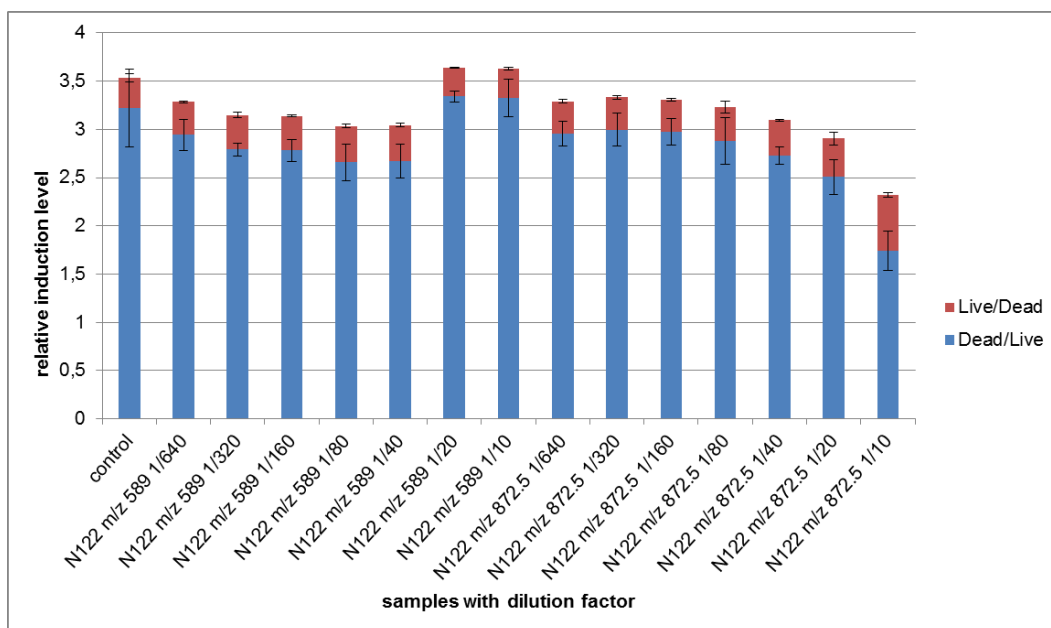


Figure 11 Measurement of Cytotoxicity of cyanobacterial compound N122 m/z 872.5 with Multitox-Fluor™.

In Figure 12 the detergent Digitonin was used as control and several crude extracts were tested for cytotoxicity in combination with an Caspase 3/7 assay. The samples NMB and De showed a high cytotoxicity compared to the control, the sample N14 is not toxic but shows a reduced Caspase 3/7 induction level compared to the control. The sample C24 is toxic and the level of Caspase 3/7 is reduced. The combination of the cytotoxicity measurement with the Caspase 3/7 measurement in the Multitox-Fluor™ Assay is a promising method to evaluate the therapeutical potential of test substances.

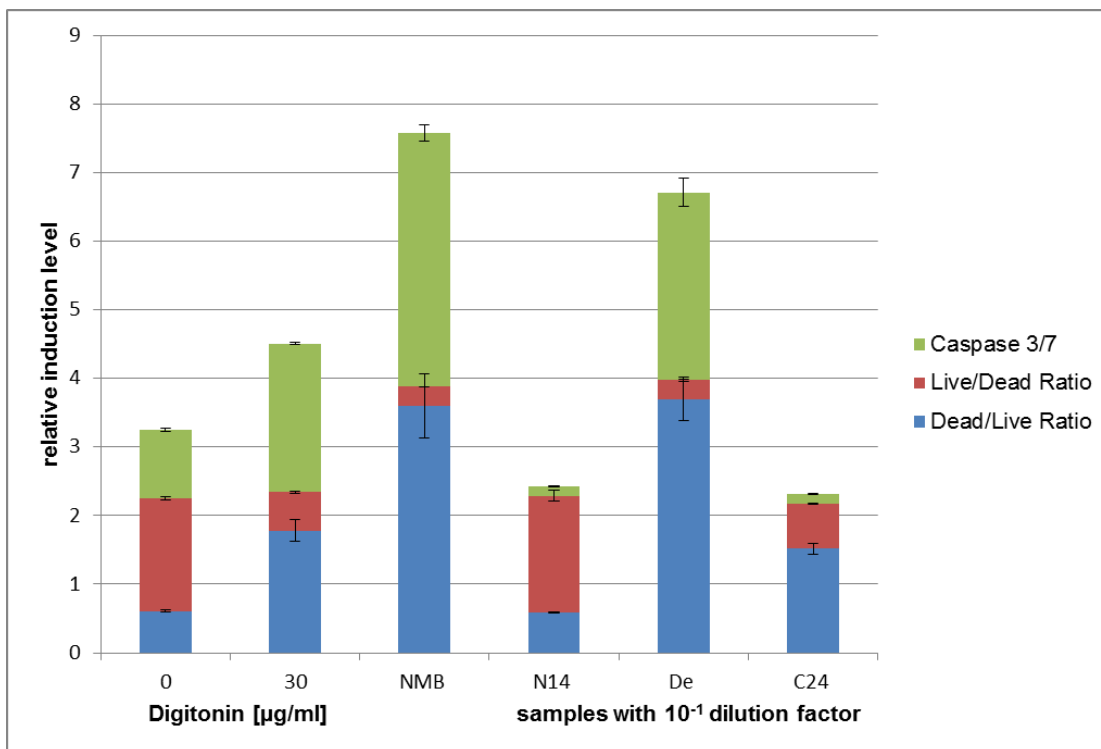


Figure 12 Cytotoxicity measurement of several crude extracts isolated from cyanobacteria

### ECIS Experiment

For the measurement of the cell monolayer integrity and the viability we plated HLMVEC, incubated them overnight and treated the cells with medium only as negative control or with TritonX-100 as positive control. Therefore we used dilutions from 0.000625%, 0.00125% to 0.005% of TritonX-100. We measured the impedance (ohm) at 4000 Hz for 24 h. As shown in Figure 13, Triton-X100 had dose-dependent effects to the cell monolayer integrity and emerged to be a good positive control substance.

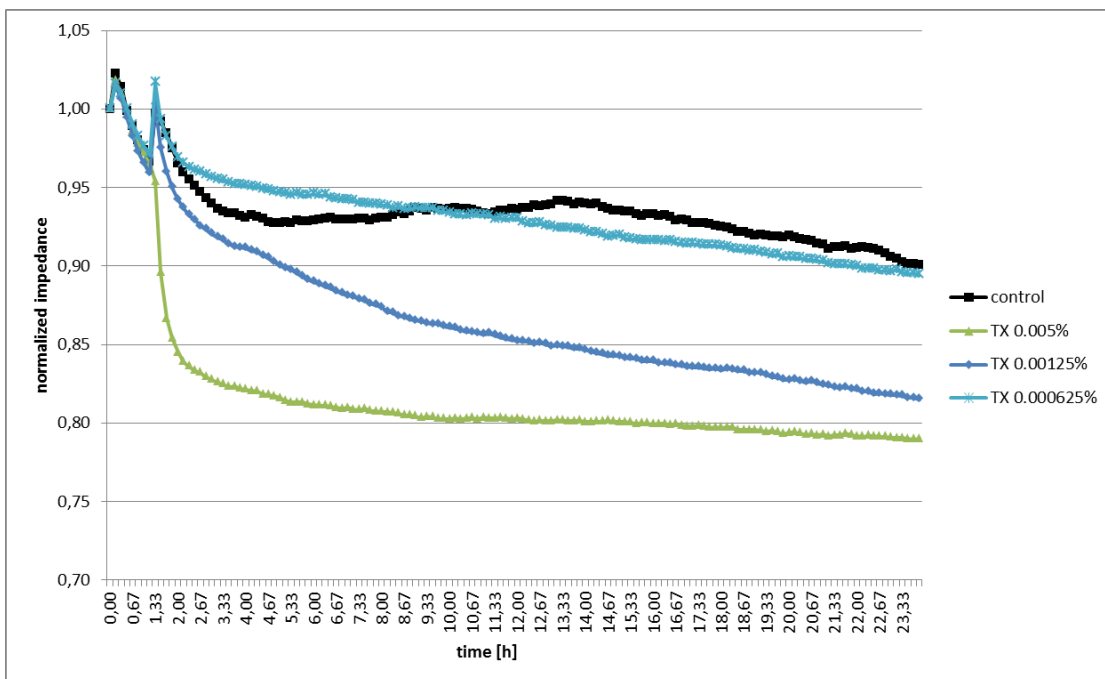


Figure 13 Measurement of the impedance after TritonX-100 treatment.

Moreover we tested several cyanobacterial compounds (Nostoc) for cytotoxic and the endothelial cell monolayer integrity concerning effects. As shown in Figure 14 the Nostoc sp. No.17 m/z 1081 shows no cytotoxic effects but a barrier-protective effect compared to the control.

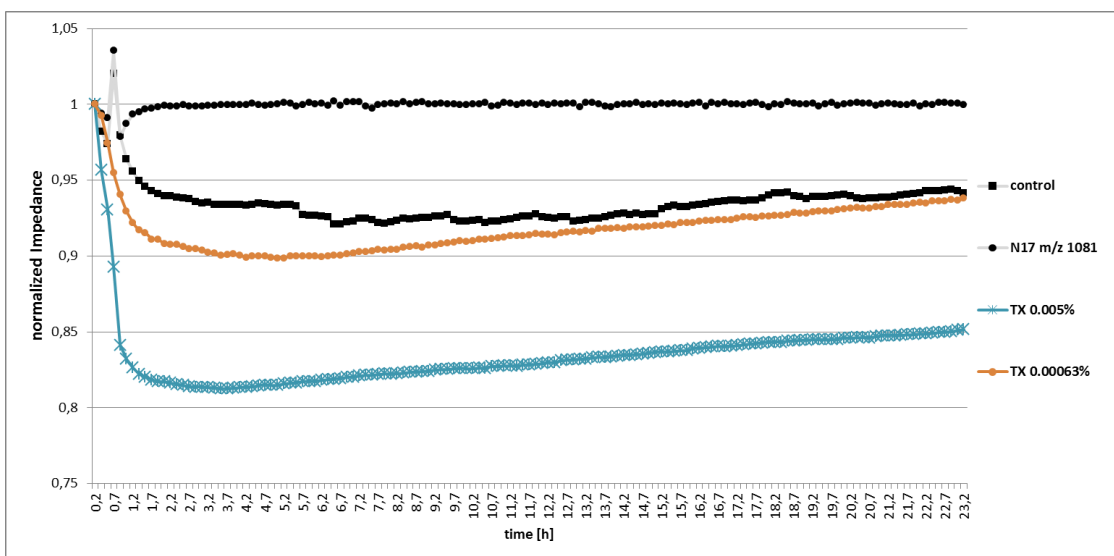


Figure 14 Measurement of the impedance after stimulation of HLMVECs with Nostoc sp. No.17



## CellSensor® Cell-Based Pathway Analysis Assays

### LiveBlazer™ Nf-κB Assay

As positive control we used hTNF in the concentration range 0.01 ng.ml<sup>-1</sup> to 10 ng.ml<sup>-1</sup>. The test substances are stimulated with 0.4 ng.ml<sup>-1</sup> hTNF after 30 min pre-incubation. Comparing the Nf-κB Level of 0.4 ng.ml<sup>-1</sup> of hTNF with the Nostoc sp. No. 17 in Figure 15 there is a concentration dependent inhibition of Nf-κB for the dilution factor from 1/10 to 1/40 for m/z 1081 and from 1/10 to 1/20 for m/z 865.5.

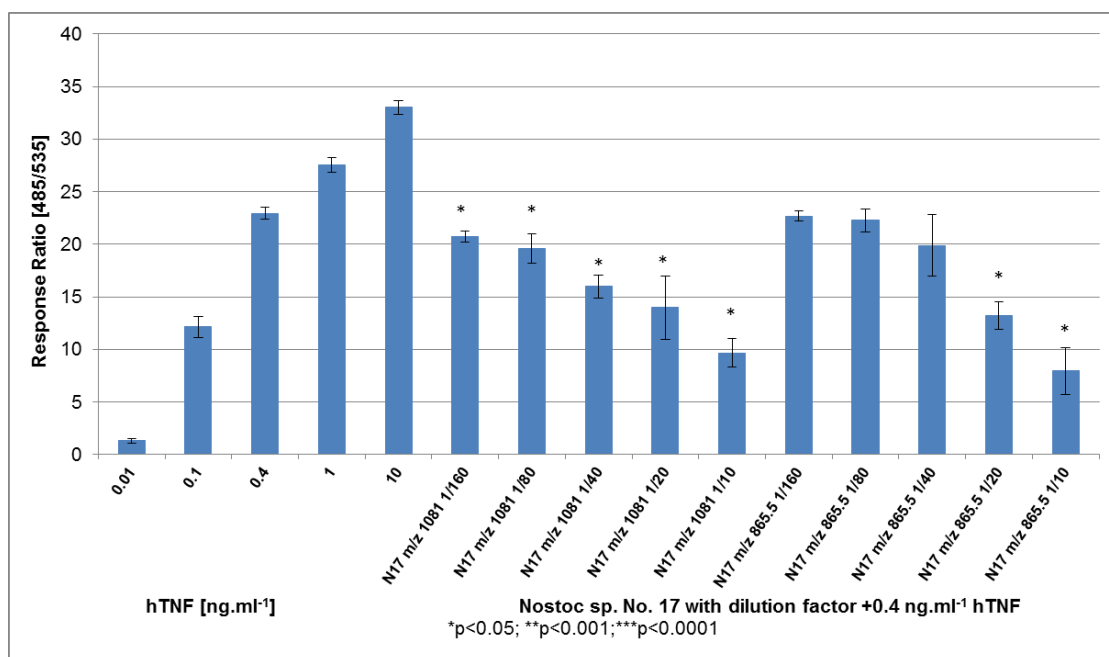


Figure 15 Response Ratio of Nf-κB stimulated with Nostoc sp. No. 17

In Figure 16 we tested the compound Nostoc muscorum No.30 F5 for the dilution factor from 1/10 up to 1/100 and we saw an Nf-κB downregulation for the dilutions 1/10 up to 1/30 continued by a constant downregulated Nf-κB level up to the 1/100 dilution.

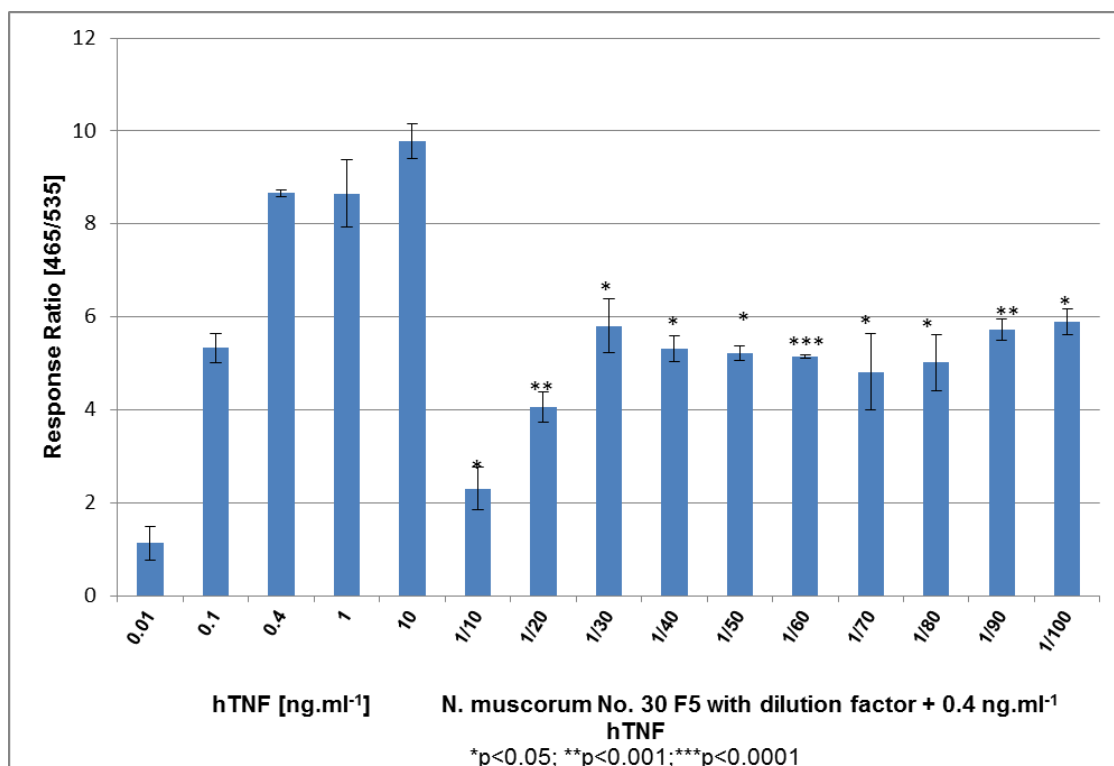


Figure 16 Response Ratio of Nf-κB stimulated with Nostoc muscorum No.30

In Figure 17 we tested Nostoc sp. No.8 m/z 721.6 for Nf-κB inhibition capabilities. We pre-incubated the cells with 1, 0.1, 0.001 and 0.0001 ng.ml<sup>-1</sup> of the compound and determined the strongest Nf-κB inhibition with 1 ng.ml<sup>-1</sup> decreasing with lower concentration of the compound.

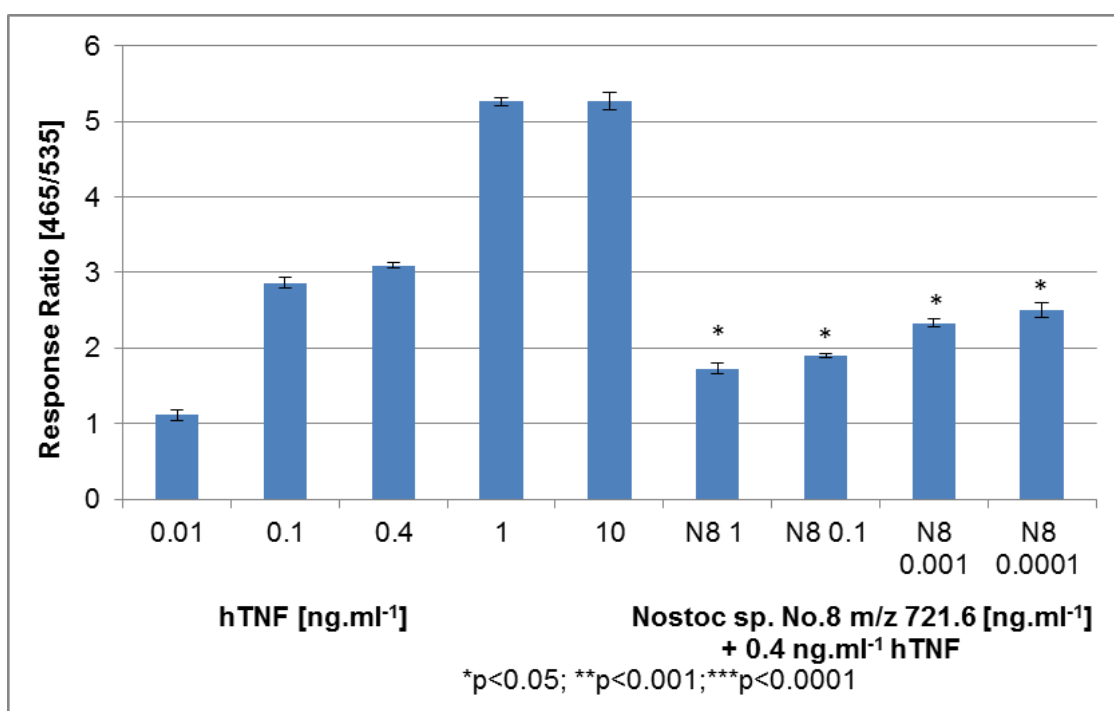


Figure 17 Response Ratio of Nf-κB stimulated with Nostoc sp. No.8

## LanthaScreen™ IκB Assay

In this experiment we pre-incubated fractions of *Nostoc* sp. De No. 114 for 30min, then we stimulated with 1 ng.ml<sup>-1</sup> of hTNF. In this experiment the three fractions of *Nostoc* sp. De No. 114 with m/z 781.8, m/z 803.7 + 823.8 + 805.9 + 823.8 and m/z 789.8 + 807.8 downregulate the IκB level significant compared to the IκB level of 1 ng.ml<sup>-1</sup> of hTNF (Figure 18).

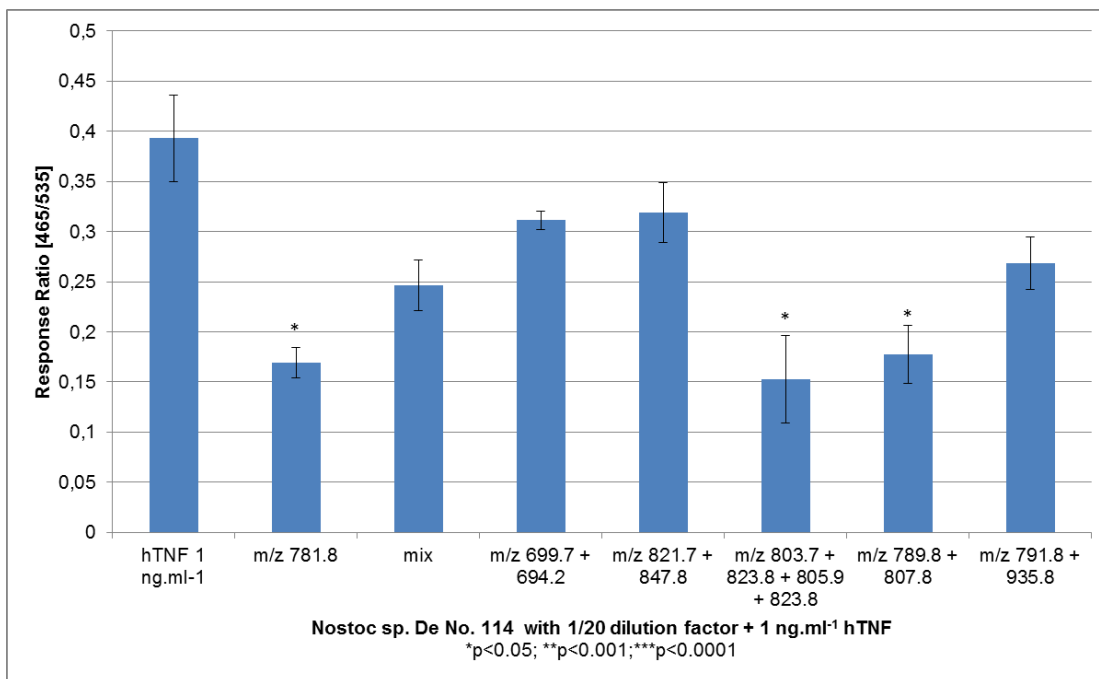


Figure 18 Response Ratio of IκB after treatment with *Nostoc* sp. De No. 114.

In the experiment in Figure 19 *Nostoc* sp. No. 17 was tested for IκB inhibitory effects. Therefore the fractions m/z 865.5 and 829.5 were tested from the 1/10 dilution up to 1/640 dilution. The fraction m/z 865.5 showed a strong IκB inhibitory effect at the 1/10 dilution. There is a IκB inhibition at all dilutions although just some are significant. Also the fraction m/z 829.5 showed a significant IκB inhibition throughout all dilutions but without any concentration dependency.

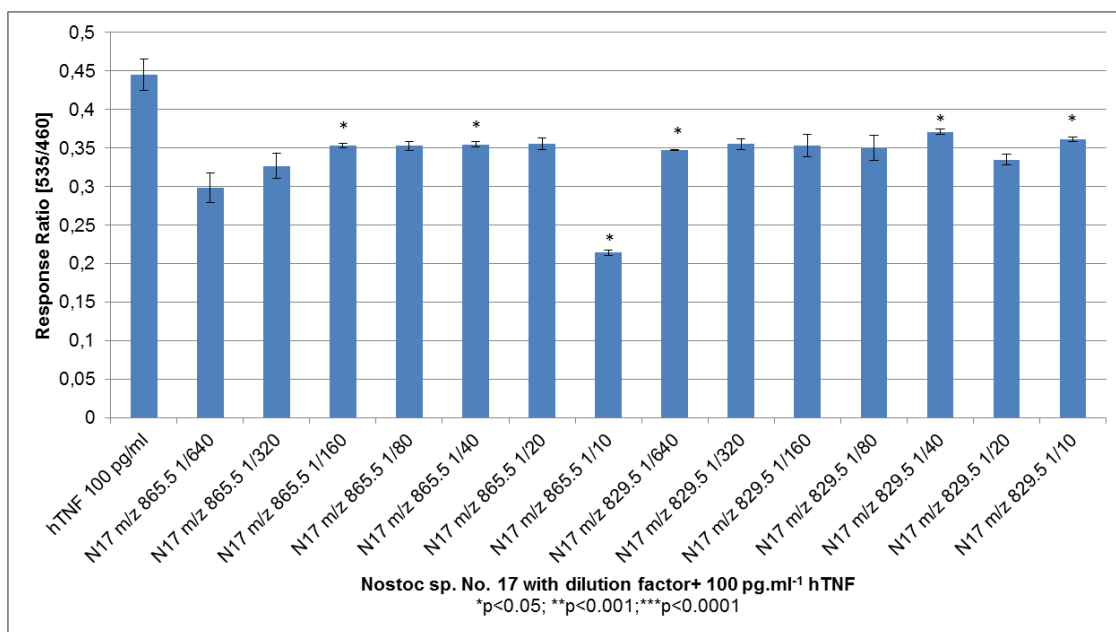


Figure 19 Response Ratio of IκB after treatment with Nostoc sp. No. 17

In Figure 20 this experiment we tested Nostoc sp. No.8 fraction m/z 721.6, m/z 899.7, m/z 885.7 and m/z 1119.8 for IκB inhibitory effects. As shown in Figure 20, no IκB inhibitory effects for this fractions can be determined by this experiment.

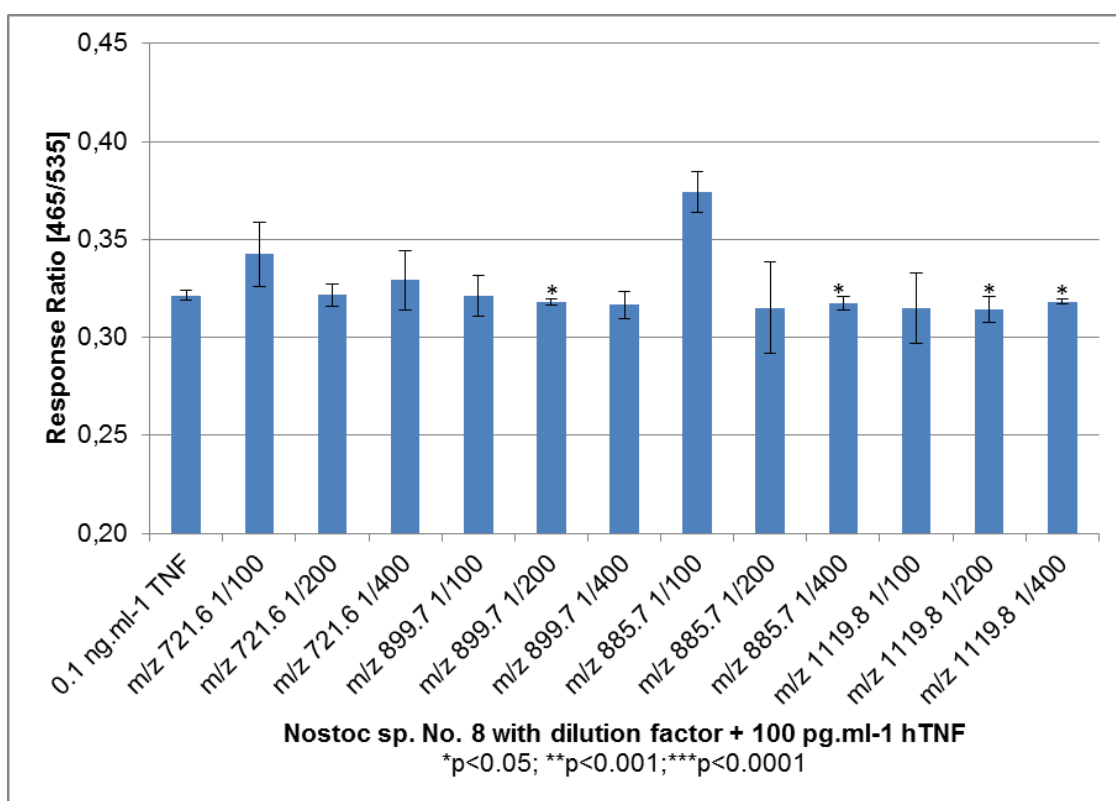


Figure 20 Response Ratio of IκB after treatment with Nostoc sp. No.8

## ICAM-1 Elisa

In this experiment we pre-incubated with several unknown samples for a concentration of 500 ng.ml<sup>-1</sup> up to 10 µg.ml<sup>-1</sup> for 30 min then we stimulated with 10 ng.ml<sup>-1</sup> hTNF. As shown in Figure 21 sample 7 as well as sample 2 showed a significant ICAM-1 inhibition.

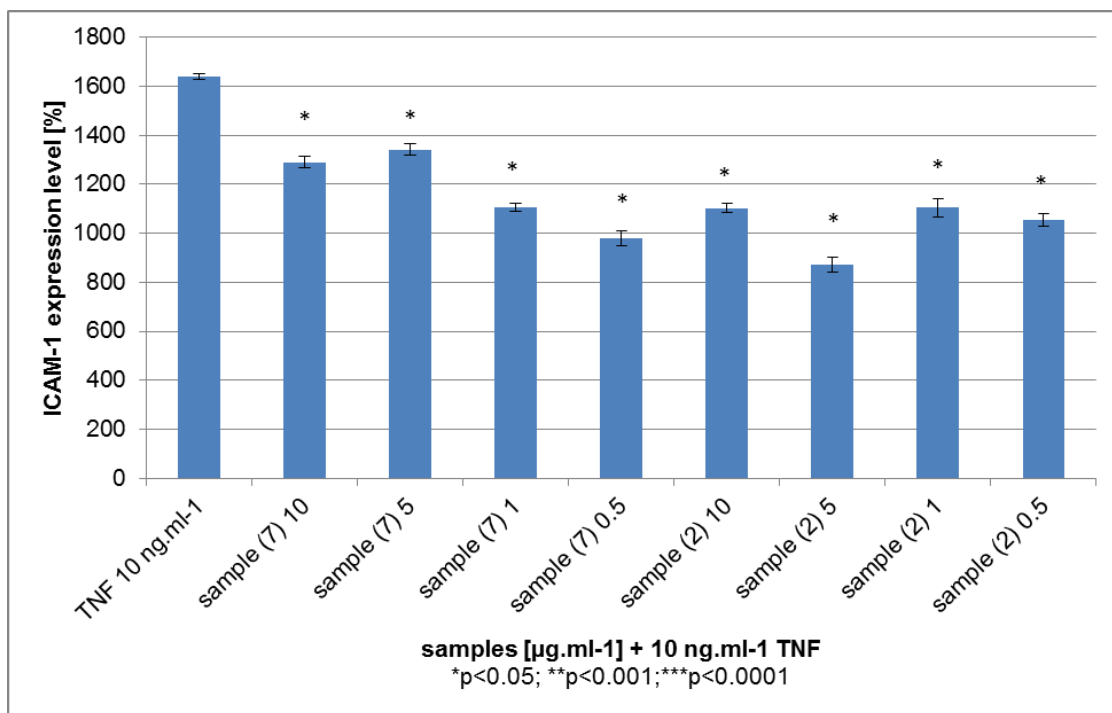


Figure 21 ICAM-1 measurements of unknown sample 7 and sample 2

In Figure 22 the unknown sample 4 and 5 were tested for ICAM-1 inhibitory effects. We saw for sample 4 at the highest concentration of 1 µg.ml<sup>-1</sup> a significant downregulation of ICAM-1 but not so for sample 5.

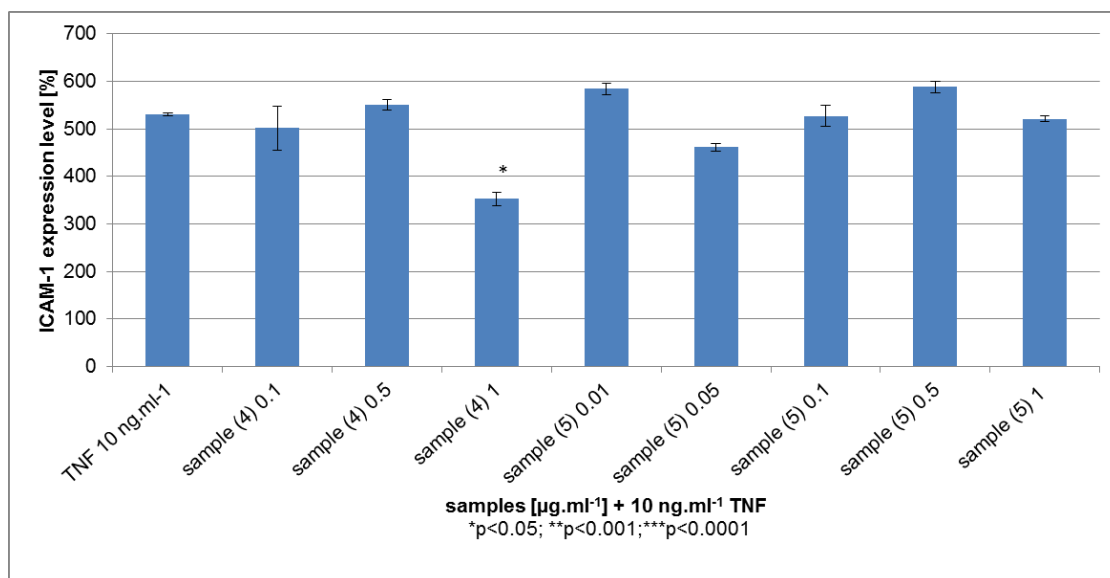


Figure 22 ICAM-1 measurement of unknown sample 4 and 5

### AlphaLisa® Assay

To evaluate the reproducibility and robustness of the AlphaLisa® Assay we compared in a 384 well plate 58 wells unstimulated with 58 wells stimulated with 100 pg.ml<sup>-1</sup> of TNF. As control we pre-incubated additional 58 wells with the p38 MAPK inhibitor SB203580 and stimulated this wells subsequently with 100 pg.ml<sup>-1</sup> TNF. SB203580 belongs to the group of pyridinyl imidazole inhibitors and is known to possess anti-inflammatory effects (24). The mean signal (%) of the negative control was 100%, with a standard deviation of 7.7%. For the positive control, the mean signal was 502.2%, with a standard deviation of 32.4%. For the p38 inhibitor/hTNF-treated control, the mean signal was 99.2%, with a standard deviation of 19.1% (Figure 23). The calculated Z-factor was 0.70, which indicates a good quality of the assay.

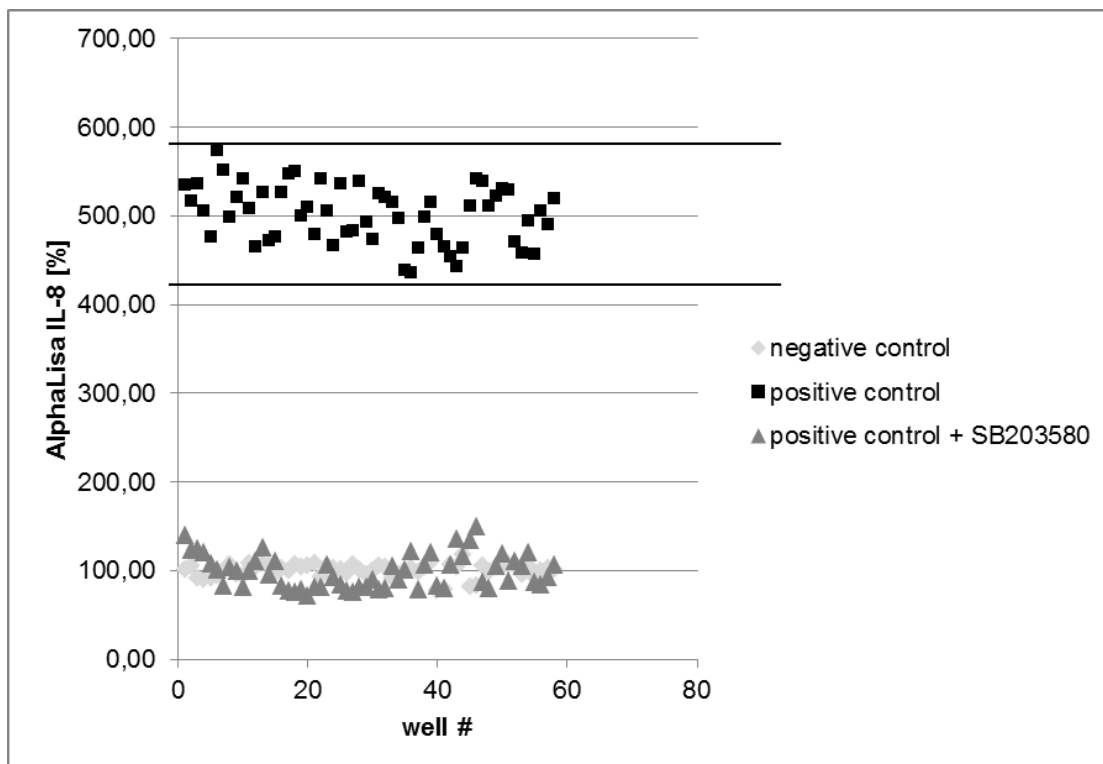


Figure 23 Evaluation of Z-factor for the AlphaLisa® IL-8 Assay

For the kinetic measurement (Figure 24) of the AlphaLisa® Assay, we incubated the HLMVEC cells with the TNF concentrations 10 pg.ml<sup>-1</sup>, 100 pg.ml<sup>-1</sup>, 1 ng.ml<sup>-1</sup> and 10 ng.ml<sup>-1</sup> and measured IL-8 and ICAM-1 after 4 h, 12 h, 18 h or 24 h. In Figure 24 an increasing production of the cytokines IL-8 and ICAM-1 corresponding to the time is shown.

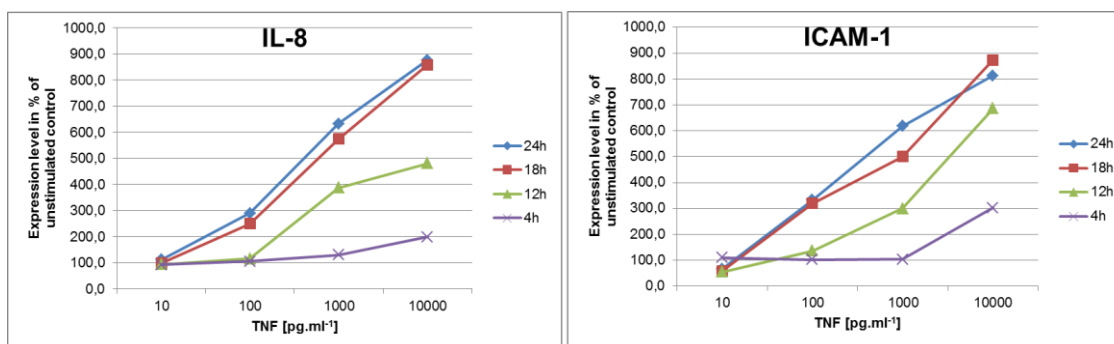


Figure 24 Kinetic measurement of hTNF

For the validation of the AlphaLisa® Assay, we made a dose-response curve (Figure 25) with the p38 MAPK inhibitor SB203580, therefore we pre-incubated the HLMVEC with SB203580 for 30 min, then we stimulated the cells with a TNF concentration of 100 pg.ml<sup>-1</sup>. For ICAM-1 an IC<sub>50</sub> of 82 μM could be calculated.

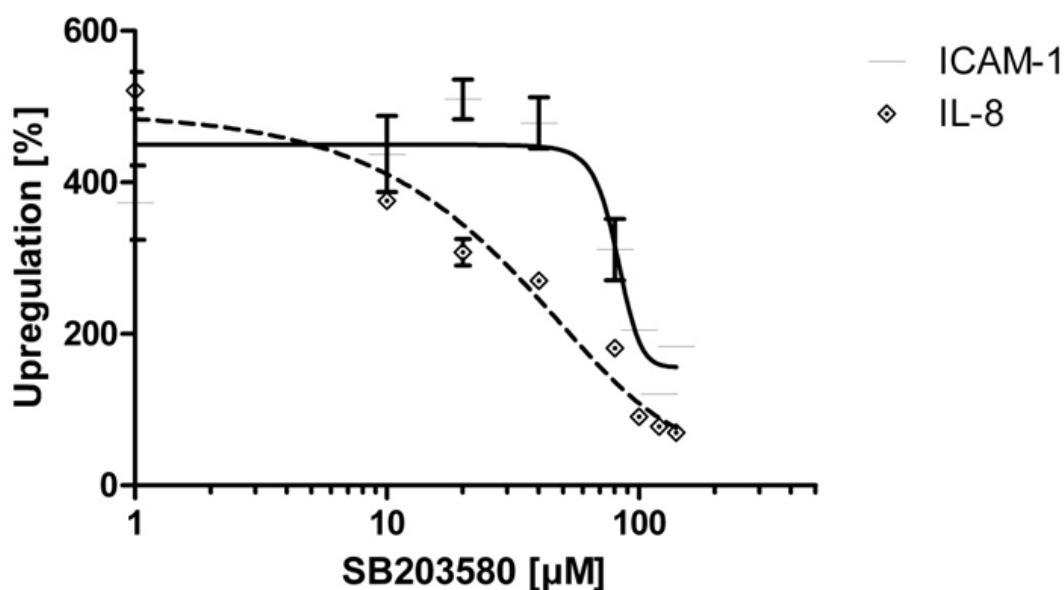


Figure 25 AlphaLisa detected inhibition of TNF stimulation with SB203580

To determine the optimal concentration of TNF for the stimulation of human lung microvascular endothelial cells, they were treated with various concentrations of the cytokine TNF. In addition, a bovine serum albumin (BSA) control was used to exclude unspecific binding of proteins to beads. There are no significant changes of the BSA control compared with TNF 400 pg.ml<sup>-1</sup> (see Figure 26).

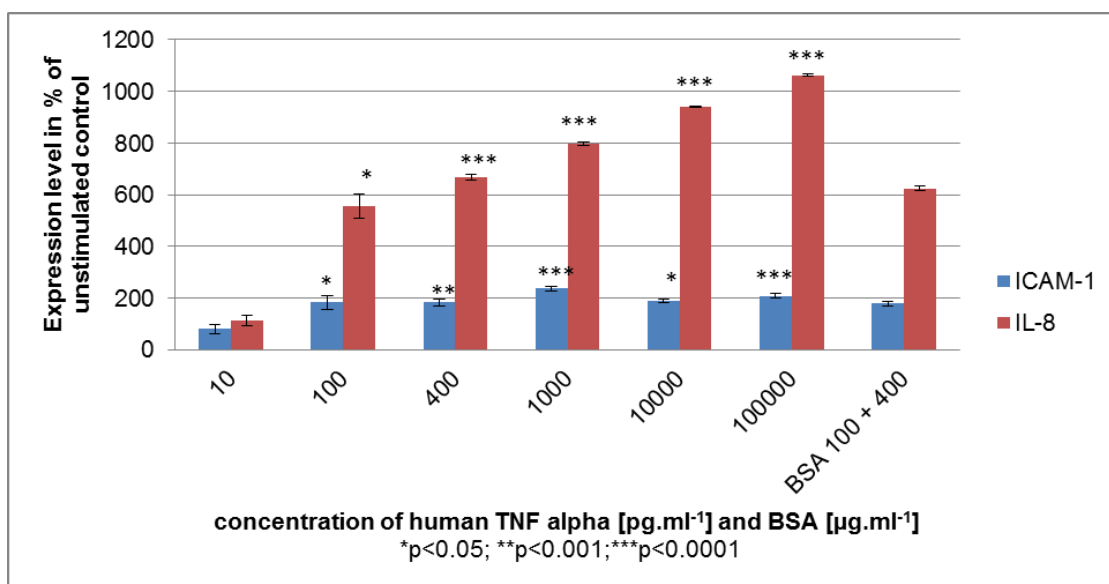


Figure 26 Responsiveness of HLMVEC to TNF in AlphaLisa assay



In experiment in Figure 27 we tested the bioactive substance N17 m/z 1081 for ICAM-1 and IL-8 expression after pre-stimulation with the fraction and subsequently stimulation with 100 pg.ml<sup>-1</sup> TNF. The two fractions are two variants of the nostopeptolides A, a group of natural toxins (30). These fractions were able to reduce IL-8 levels from 600% to 300% and ICAM-1 levels in supernatants from 300% to 100%.

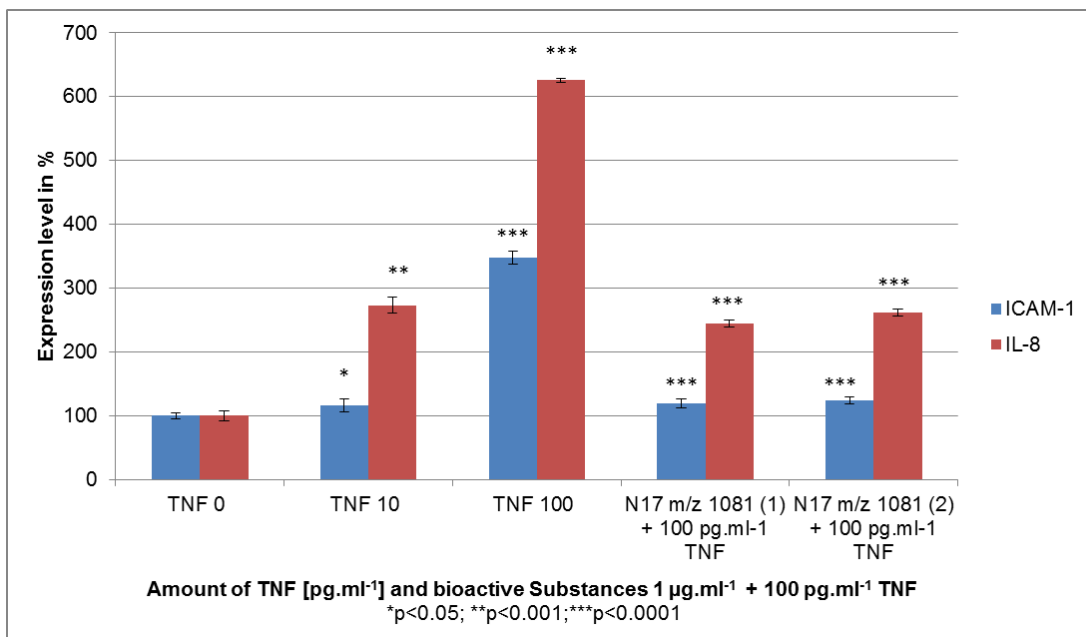


Figure 27 ICAM-1 and IL-8 expression level of Nostoc sp. No. 17

In Figure 28 the ICAM-1 expression was measured of several fractions of *Nostoc* sp. De No.114, *Nostoc* sp. No.8 and No.17. After pre-incubation of HLMVEC with the fractions for 30 min the cells were subsequently stimulated with  $0.4 \text{ ng.ml}^{-1}$  of TNF. In the experiment shown in Figure 28 especially the fraction *Nostoc* sp. No.8 m/z 721.6 shows a significant ICAM-1 inhibition of  $174\% \pm 6.7\%$  compared to  $0.4 \text{ ng.ml}^{-1}$  TNF.

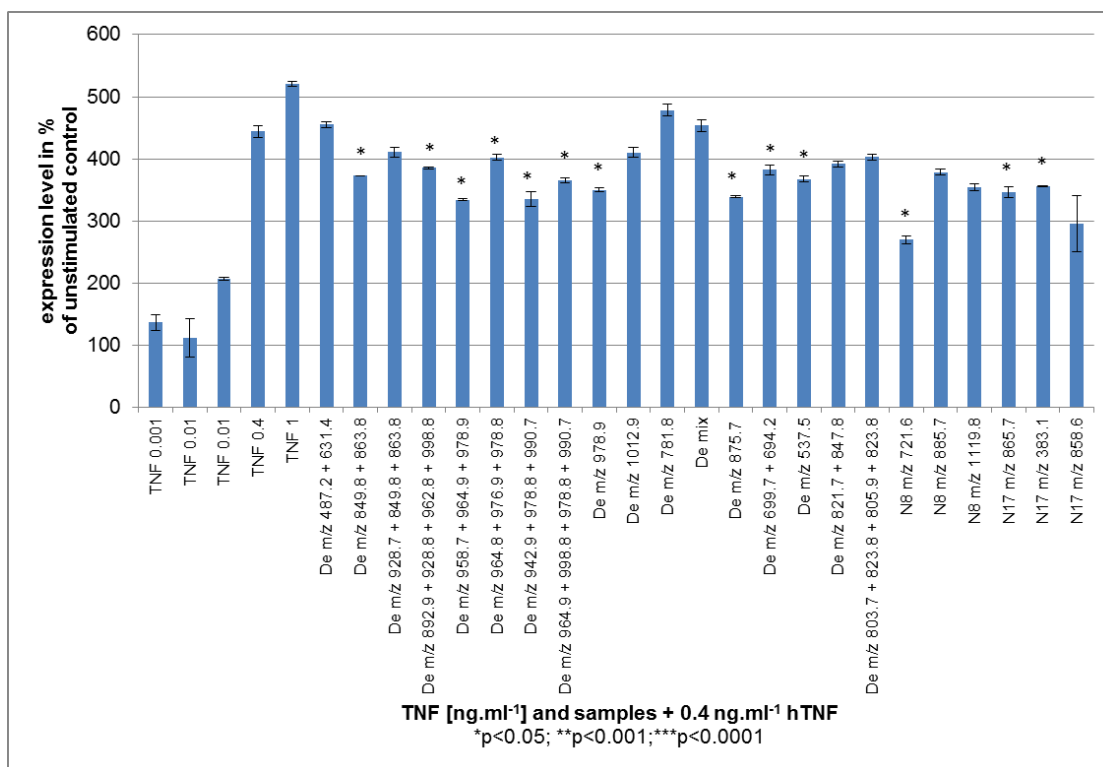


Figure 28 ICAM-1 measurement of several compounds

## Nf-κB nucleus translocation

For the Nf-κB translocation experiment we used the SB203580 inhibitor as Nf-κB inhibitor. As shown in Figure 29 this control inhibitor clearly inhibited the Nf-κB translocation into the nucleus. The Nostoc sp. No.17 m/z 865.5 fraction also inhibited at a concentration of 1 μg.ml<sup>-1</sup> the Nf-κB translocation whereas the TNF 0.1 ng.ml<sup>-1</sup> concentration alone was leading to a Nf-κB translocation into the nucleus.

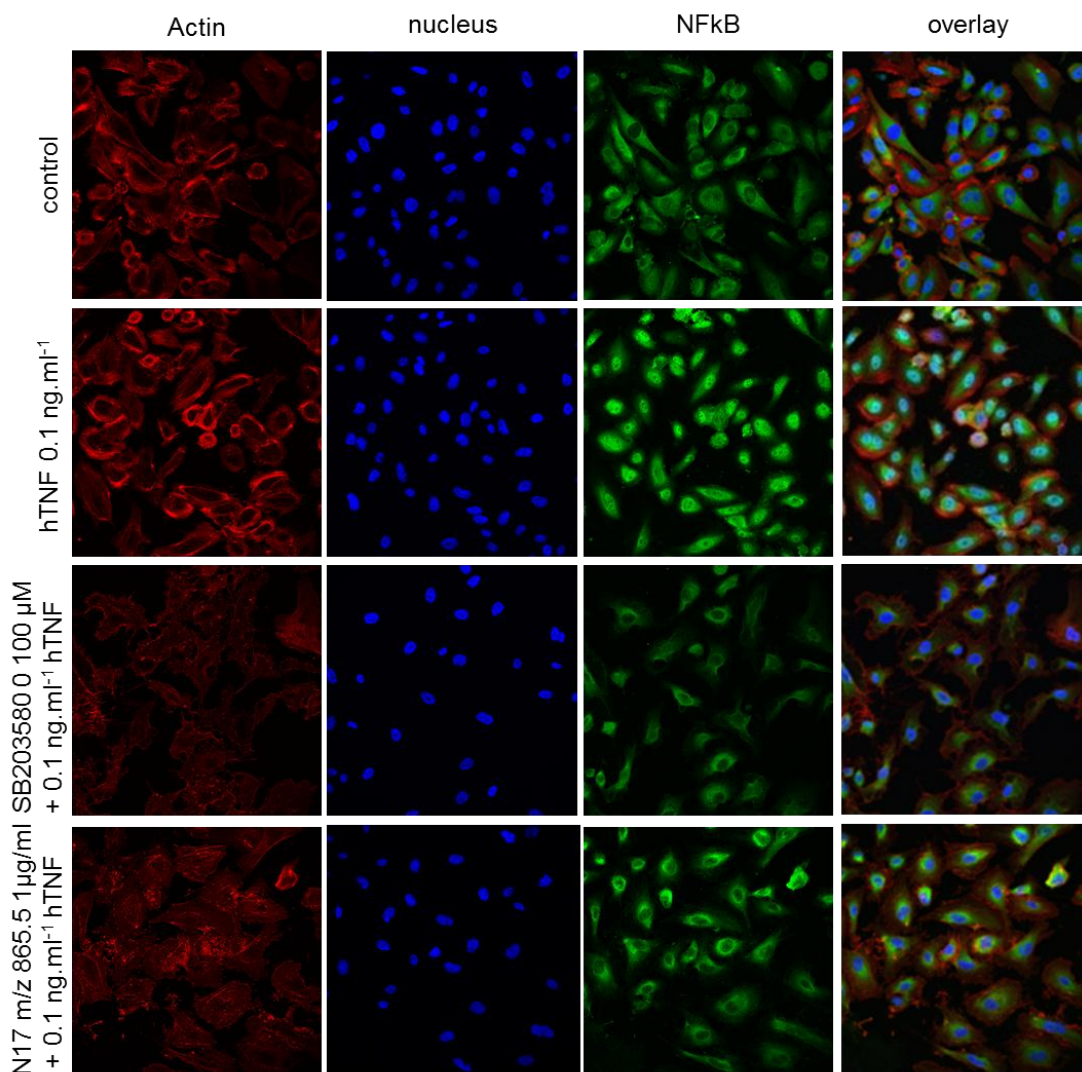


Figure 29 Nuclear translocation of NFκB in Huvec cells

### 3D Artificial skin model – wound healing

The artificial skin was prepared and treated with several substances. After 6 h the measurement of the fibroblasts is shown in Figure 30. Though there are high standard deviations, some substances seem to have pro-migration activities. In this experiment, especially sample No. 18, 19, 20, 23, 24, 32, 60, 66, 143 and 144 turned out to promote migration significantly compared to the unstimulated control.

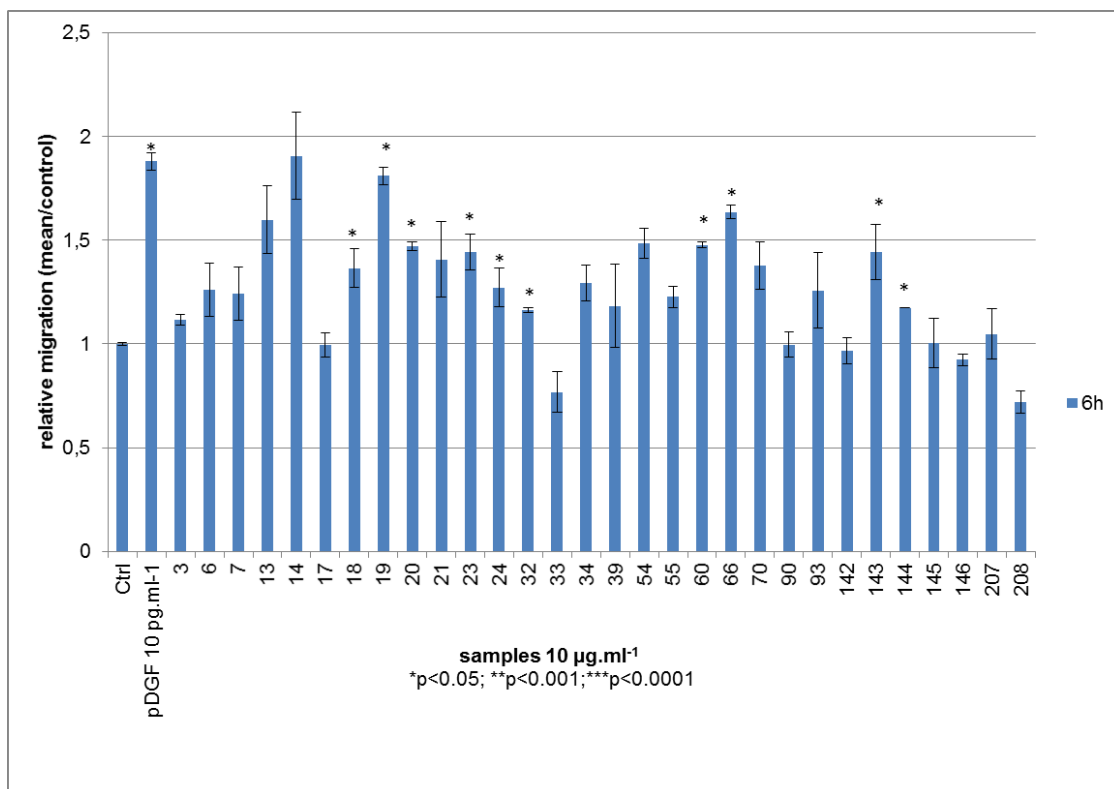


Figure 30 Treatment of artificial skin with several substances

## Discussion

Bioactive substances, isolated from nature are a promising source of compounds for the pharmaceutical industry. The pre-selection of bioactivity is already done by environmental evolution which is an advantage compared to the time consuming random screening of synthetic drugs. High-throughput assays that are able to identify and characterize bioactive substances are the workhorse for their routine-based search. With this study comparing and characterizing commercial assays for their ability to test substances for cytotoxicity, anti-inflammatory or wound healing effects in high-throughput assays we contribute to the establishment of novel test systems for standardized screening of bioactive substances. Our results demonstrate the potential identification of promising anti-inflammatory substances, which could further be tested in in vivo models. Because compounds are tested early and in real time in pathologically relevant primary human cells, cytotoxic and barrier-disintegrating side effects can be detected at an early phase of preclinical research. Details of the individual test systems can be summed up as follows:

### Testing Cytotoxicity of natural isolated substances

For the identification of bioactive compounds the exclusion of cytotoxic substances is essential. We compared several Cytotoxicity assays and we were able to evaluate the cytotoxicity of natural substances in all tested assays exact and reliable. The combination of a Cytotoxicity assay with the measurement of the Caspase 3/7 levels when using the Multitox-Fluor™ assay gives new important information but raises the costs for the assays especially if a scale up to high throughput screening should be conducted. The ECIS experiment has the advantage that also an improvement of the monolayer integrity can be measured beside the toxicity but just a few compounds can be tested in one experiment due to the sextuple replicates done in the experiment. We tested the robustness of this assay using the detergent Triton X-100 in several concentrations as control. With this assay we found the

cyanobacterial compound (N17 m/z 1081, see Figure 14) with barrier protective effects.

#### Testing CellSensor® Cell-Based Pathway Analysis Assays

With this assays it is possible to detect the cellular pathway mechanism of the test substances. We tested the Nf-κB pathway and the IκB pathway. The compounds were isolated at the Institute of Microbiology, Academy of Science, in the Czech Republic and purified (30). We have tested 78 different cyanobacterial extracts and purified metabolites in various concentrations for Nf-κB or IκB inhibitory activities after exclusion of cytotoxic compounds. In several fractions of Nostoc sp. No. 17, Nostoc muscorum No.30, Nostoc sp. No.8 and Nostoc sp. De No. 114 we were able to find auspicious compounds. We evaluated this CellSensor® Cell-Based Pathway Analysis Assay as a reliable and reproducible for testing of natural substances. The main advantage of this assay is that it's possible to detect the pathway mechanism of a bioactive compound.

#### Detection of cytokine expression with ELISA and AlphaLisa® Assays

Unlike the most cell-based enzyme-linked immunosorbent assays the AlphaLisa® Assays don't require fixation of cells and several washing steps for removing unbound primary and secondary antibodies. These manipulation steps can potentially lead to high variations in cell numbers in individual wells of the microplate, which can hinder the evaluation of the results. Although all experiments were done by manual pipetting in 384-well plates, only small standard deviations were observed. From these data, we conclude that the AlphaLisa® Assay has a good potential to be performed in a fully automated HTS environment. The average Z-factor value of the assay was greater than 0.7 (for AlphaLISA), indicating it could be further adapted from the 384-well to a 1536-well format.

#### Nf-κB nucleus translocation

Compounds proved for Nf-κB inhibition in the CellSensor® Cell-Based Pathway Analysis Assay were observed microscopically for Nf-κB nucleus translocation. With this assay we were able to confirm the Nf-κB inhibitory effect of Nostoc sp. No. 17 m/z 865.5. With this assay we were able to confirm the results of the CellSensor® Cell-Based Pathway Assay and the detected Nf-κB inhibitors.

### 3D Artificial skin model – wound healing

For the 3D Artificial skin model the Oris Cell Migration Assay was used to build up a 3 dimensional environment. In this artificial skin model the different cell types fibroblasts, endothelial cells and keratinocytes can interact with each other which is important for the exact characterization of biological compounds for there wound healing activity. We saw high standard deviation in this assays due to the artificial skin modelling in the 96 well plate this assay but in our experiments we were able to find some wound healing promoting substances.

## References

1. **Alejandro M.S. Mayer, Ph.D. (1999)** *Marine Pharmacology in 1998: Antitumor and Cytotoxic Compounds*, *The Pharmacologist* 41:159-164
2. **Ira Bhatnagar and Se-Kwon Kim (2010)** Immense Essence of Excellence: Marine Microbial Bioactive Compounds, *Marine Drugs*, 8(10):2673-701
3. **David J. Newman and Gordon M. Cragg (2007)** Natural Products as Sources of New Drugs over the Last 25 Years. *Journal of Natural Products*, 70(3):461-77
4. **Aishwarya V. Ramaswamy, Patricia M. Flatt, Daniel J. Edwards, T. Luke Simmons, Bingnan Han and William H. Gerwick (2006)** The Secondary Metabolites and Biosynthetic Gene Clusters of Marine Cyanobacteria. Applications in Biotechnology, *Frontiers in Marine Biotechnology*, 5:175-223
5. **Adam C. Jones, Liangcai Gu, Carla M. Sorrels, David H. Sherman, and William H. Gerwick (2010)** New Tricks from Ancient Algae: Natural Products Biosynthesis in Marine Cyanobacteria, *Current Opinion in Chemical Biology*, 13(2):216-223
6. **George E. Chlipala, Shunyan Mo, and Jimmy Orjala (2011)** Chemodiversity in Freshwater and Terrestrial Cyanobacteria – a Source for Drug Discovery. *Current Drug Targets*, 12(11): 1654–1673
7. **Susanne Grabley Ralf Thiericke (1999)** Bioactive Agents from Natural Sources: Trends in Discovery and Application, *Advances in Biochemical Engineering*, 64:101-154
8. **D. A. Pereira, J. A. Williams (2007)** Origin and evolution of high throughput screening, *British Journal of Pharmacology*, 152(1):53-61
9. **WHO (2011)** Cancer, *World Health Organization, Fact sheet N°297*
10. **WHO (2008)** Cause-specific mortality, *World Health Organization*, 1: 1-28
11. **Douglas Hanahan and Robert A. Weinberg (2011)** Hallmarks of Cancer: The next Generation, *Cell*, 144(5):646-74
12. **Francesco Colotta, Paola Allavena, Antonio Sica, Cecilia Garlanda and Alberto Mantovani (2009)** Cancer-related inflammation, the seventh hallmark of cancer: links to genetic instability, *Carcinogenesis*, 30(7):1073-81
13. **Bharat B. Aggarwal, Shishir Shishodia, Santosh K. Sandur, Manoj K. Pandey, Gautam Sethi.** Inflammation and Cancer: how hot is the link? *biochemical pharmacology*. 2006.
14. **Baharat B., Subash C. and Ji Hye Kim (2011)** Historical perspectives on tumor necrosis factor and its superfamily:25 years later, a golden journey, *Blood*, 119(3):651-65
15. **M. Ocker, M. Höpfner (2012)** Apoptosis-Modulating Drugs for Improved Cancer Therapy, *European Surgical Research*, 48(3):111-20
16. **Bradley, JR (2008)** TNF-mediated inflammatory disease, *Journal of Pathology*, 214(2):149-60
17. **Pascal Schneider, Fabienne MacKay, Véronique Steiner, Kay Hofmann, Jean-Luc Bodmer, Nils Holler, Christine Ambrose, Pornsri Lawton, Sarah Bixler, Hans Acha-Orbea, Danila Valmori, Pedro Romero, Christiane Werner-Favre, Jeffrey L. Browning and Jürg Tschopp (1999)** BAFF, a Novel Ligand of the Tumor Necrosis Factor Family, Stimulates B Cell Growth, *The Journal of Experimental Medicine*, 189(11):1747-56



18. **Yulia N. Demchenko and W. Michael Kuehl (2010)** A critical role for the NFkB pathway in multiple myeloma, *Oncotarget*, 1(1):59-68
19. **Shin Maeda and Masao Omata (2008)** Inflammation and cancer: Role of nuclear factor-kappaB activation, *Cancer Science*, 99(5):836-42
20. **Beatrice Rayet and Celine Gelinas (1999)** Aberrant rel/nfkb genes and activity in human cancer, *Oncogene*, 18(49):6938-47
21. **Florence Folmer, Marcel Jaspers, Mario Dicato, Marc Diederich (2008)** Marine natural products as targeted modulators of the transcription factor NF-kB, *Biochemical Pharmacology*, 75(3):603-17
22. **Yi-Feng Xia, Bu-Qing Ye, Yi-Dan Li, Jian-Guo Wang, Xiang-Jiu He, Xianfeng Lin, Xinsheng Yao, Dawei Ma, Arne Slungaard, Robert P. Hebbel, Nigel S. Key and Jian-Guo Geng (2010)** Andrographolide Attenuates Inflammation by Inhibition of NF-kB Activation through Covalent Modification of Reduced Cysteine 62 of p50, *The Journal of Immunology*, 173(6):4207-17
23. **Doris R. Siwak, M.S., Shishir Shishodia, Ph.D., Bharat B. Aggarwal, Ph.D., Razelle Kurzrock, M.D. (2005)** Curcumin-Induced Antiproliferative and Proapoptotic Effects in Melanoma Cells Are Associated with Suppression of Ikb Kinase and Nuclear Factor kB Activity and Are Independent of the B-Raf/Mitogen-Activated/Extracellular Signal-Regulated Protein Kinase Path, *Cancer*, 104(4):879-90
24. **Florence Folmer, Marcel Jaspers, Mario Dicato, Marc Diederich (2007)** Marine natural products as targeted modulators of the transcription factor NF-kB, *Biochemical Pharmacology*, 75(3):603-17
25. **Kazuhiro Ashikawa, Sekhar Majumdar, Sanjeev Banerjee, Alok C. Bharti, Shishir Shishodia and Bharat B. Aggarwal (2002)** Piceatannol Inhibits TNF-Induced NF-kB activation and NF-kB-mediated gene expression through Suppression of I kB  $\alpha$  kinase and p65 phosphorylation, *The Journal of Immunology*, 169(11):6490-7
26. **Richard M. Eglén, Terry Reisine, Philippe Roby, Nathalie Rouleau, Chantal Illy, Roger Boss (2008)** The Use of AlphaScreen Technology in HTS: Current Status, *Current Chemical Genomics*, 1:2-10
27. **Sciences, PerkinElmer Life and Analytical (2004)** Practical Guide to working with AlphaScreen, *PerkinElmer*, PerkinElmer LAS literature 007011\_01:1-60
28. **Life Technologies (2006)** *LiveBlazer™ FRET - B/G Loading Kit protocol*, (1): 1-10
29. **COBY B. CARLSON, MATTHEW B. ROBERS, KURT W. VOGEL, THOMAS MACHLEIDT.** Development of LanthaScreen™ Cellular Assays for Key Components within the PI3K/AKT/mTOR Pathway. *Journal of Biomolecular Screening*. 2009, 121-132.
30. **Maren Pflüger, Aleksandra Kapuscik, Rudolf Lucas, Anita Koppensteiner, Michael Katzlinger, Jouni Jokela, Andreas Eger, Nico Jacobi, Christoph Wiesner, Elisabeth Hofmann, Kamil Önder, Jiri Kopecky, Wolfgang Schütt, and Harald Hundsberger (2013)** A Combined Impedance and AlphaLISA-Based Approach to Identify Antiinflammatory and Barrier-Protective Compounds in Human Endothelium, *Journal of Biomolecular Screening*, 18(1):67-74
31. **David J. Newman, Gordon M. Cragg, Kenneth M. Snader (2003)** Natural Products as Sources of New Drugs over the Period 1981-2002. *Journal of Natural Products*, 66(7):1022-37

32. **Zhou, Y Wu and BP (2010)** TNF- $\alpha$ /NF- $\kappa$ B/Snail pathway in cancer cell migration and invasion, *British Journal of Cancer*, 102(4):639-44
33. **C.A. Hazzalin (1996)** p38/RK is Essential for Stress-Induced Nuclear Responses: JNK/SAPKs and c-Jun/ATF-2 Phosphorylation are Insufficient, *Current Biology*, 6(8):1028-31

## Curriculum vitae

### Dipl.Biol. Maren Pflüger

Address: Herzogstrasse 11/2, A-3500 Krems an der Donau

E-mail: maren.pflueger@fh-krems.ac.at

Date of birth: 17<sup>th</sup> September 1977

Place of birth: 71229 Leonberg

Nationality: German

### Employments

---

- |                |  |
|----------------|--|
| 10.2005- now   | IMC Fachhochschule Krems<br>scientific assistant   |
| 10.2003-6.2004 | University of Konstanz,<br>biochemical pharmacology, scientific assistant<br>Prof. A. Wendel |

### Education and Further Education

---

- |                |   |
|----------------|---|
| 10.2002-9.2003 | diploma thesis: Development of an in vitro<br>angiogenesis assays for analysis of<br>human liquids.<br>mark for diploma thesis: 1 |
| 8.2000-9.2002  | University of Konstanz, biology dipl.   |
| 9.1998-7.2000  | University of Hohenheim,<br>study of biology<br>pre-degree biology  |

### Publications

---

- **The Tumor Necrosis Factor-derived TIP peptide: a potential anti-edema drug**  
Rudolf Lucas, Harald Hundsberger, Maren Pflüger, Bernhard Fischer, Denis Morel, Clemens Braun, Albrecht Wendel, Trinad Chakraborty, Wolfgang Schütt, Christoph Wiesner and Jürg Hamacher  
*Letters in Drug Design & Discovery*, 2007, Vol. 4, 336- 340
- **Endothelial Cell-Based Methods for the Detection of Cyanobacterial Anti-Inflammatory and Wound-Healing Promoting Metabolites**  
Christoph Wiesner, Jiri Kopecky, Maren Pflueger, Harald Hundsberger, Barbara Entler, Christoph Kleber, Josef Atzler, Pavel Hrouzek, Dalibor Stys, Alena Lukesova, Wolfgang

Schuett and Rudolf Lucas  
*Drug Metabolism Letters*, 2007, 1, 254-260

- **TNF: a Moonlighting Protein at the Interface between Cancer and Infection**  
Harald Hundsberger, Alexander Verin, Christoph Wiesner, Maren Pflüger, Alexander Dulebo, Wolfgang Schütt, Ignace Lasters, Daniela N. Männel, Albrecht Wendel and Rudolf Lucas  
*Frontiers in Bioscience* 5374-5386, May 1, 2008
- **Implementation of ECIS technology for the characterization of potential therapeutic drugs that promote wound-healing**  
Christoph Wiesner, Maren Pflüger, Jiri Kopecky, Dalibor Stys, Barbara Entler, Rudolf Lucas, Harald Hundsberger, Wolfgang Schütt  
*GMS Krankenhaushygiene Interdisziplinär* 2008, Vol. 3(1), ISSN 1863-5245
- **CXCL9 induces chemotaxis, chemorepulsion and endothelial barrier disruption through CXCR3-mediated activation of melanoma cells**  
S Amatschek, R Lucas, A Eger, M Pflueger, H Hundsberger, C Knoll, S Grosse-Kracht, W Schuett, F Koszik, D Maurer and C Wiesner  
*British Journal of Cancer* (2010) 00, 1– 11
- **$\alpha$ -Catulin downregulates E-cadherin and promotes melanoma progression and invasion.**  
Kreiseder B, Orel L, Bujnow C, Buschek S, Pflueger M, Schuett W, Hundsberger H, de Martin R, Wiesner C  
*Int J Cancer*. 2013 Feb 1;132(3):521-30, doi: 10.1002/ijc.27698
- **Pleiotropic neuroprotective and metabolic effects of Actovegin's mode of action**  
Machicao F, Muresanu DF, Hundsberger H, Pflüger M, Guekht A  
*J Neurol Sci*. 2012 Nov 15;322(1-2):222-7, doi: 10.1016/j.jns.2012.07.069
- **A Combined Impedance and AlphaLISABased Approach to Identify Antiinflammatory and Barrier-Protective Compounds in Human Endothelium**  
Maren Pflüger, Aleksandra Kapuscik, Rudolf Lucas, Anita Koppensteiner, Michael Katzlinger, Jouni Jokela, Andreas Eger, Nico Jacobi, Christoph Wiesner, Elisabeth Hofmann, Kamil Önder, Jiri Kopecky, Wolfgang Schütt, and Harald Hundsberger  
*Journal of Biomolecular Screening*, 2013, Vol.18, 66-73, DOI: 10.1177/1087057112458316
- **Mesalamine modulates intercellular adhesion through inhibition of p-21 activated kinase-1**  
Vineeta Khare, Alex Lyakhovich, Kyle Dammann, Michaela Lang, Melanie Borgmann, Boris Tichy, Sarka Pospisilova, Gloria Luciani, Christoph Campregher, Rayko Evstatiev, Maren Pflueger, Harald Hundsberger and Christoph Gasche  
*Biochem Pharmacol*. 2013 Jan 15;85(2):234-44, doi: 10.1016/j.bcp.2012.10.026